Solubility and Immunoblot Assay

To examine solubility of mutant myotilin, we used frozen biopsied muscles from human control subjects and from the two myotilinopathy patients, as well as TA muscles of six mice each from the wtMYOT-, mMYOT S60C-, and mMYOT R405K-expressing groups, at 14 days after electroporation. The 1.25-mm^3 specimens of muscle were lysed and homogenized in 150 μL of radioimmunoprecipitation assay buffer containing 50 mmol/L Tris-HCl (pH 7.5), 150 mmol/L NaCl, 1 mmol/L EDTA (pH 8.0), 1% Nonidet P-40, 0.5% sodium deoxycholate, 0.1% SDS, and Roche complete protease inhibitor cocktail (Roche Diagnostics). The lysates were incubated at 4°C for 20 minutes with gentle rotation, and then centrifuged at 15,000 × *g* at 4°C for 20 minutes. The supernatants and precipitates were collected, and the protein concentrations of the supernatants were determined using a protein assay kit (Bio-Rad Laboratories, Hercules, CA). Immunoblotting of the supernatant (detergent-soluble) and precipitate (detergent-insoluble) fractions was performed, as described previously.[23] Glyceraldehyde 3-phosphate dehydrogenase (GAPDH) was used as an internal standard. Immunoreactive complexes on the membranes were detected using enhanced chemiluminescence ECL Plus detection reagent (GE Healthcare, Chalfont St Giles, UK). Insolubility index was calculated as the ratio of the quantity of insoluble protein to the total quantity of proteins (the sum of soluble and insoluble proteins).

Immunoprecipitation

The 5-mm^3 specimens of frozen electroporated mouse muscles isolated at 14 days after electroporation were lysed and homogenized in 0.6 mL of radioimmunoprecipitation assay buffer. The lysates were incubated at 4°C for 20 minutes with gentle rotation, and then centrifuged at 15,000 × *g* at 4°C for 20 minutes. The supernatants were collected, and their protein concentrations were adjusted using a protein assay kit (Bio-Rad Laboratories). Immunoprecipitation was performed as described previously,[23] with agarose-conjugated anti-Myc antibody (Santa Cruz Biotechnology).

Statistical Analysis

Differences between wtMYOT-, mMYOT S60C-, and mMYOT R405K-expressing mice were analyzed with GraphPad Prism version 5 (GraphPad Software, La Jolla, CA). Comparisons among groups were performed by one-way analysis of variance with post hoc Tukey's analysis. Data are expressed as means ± SD.

Results

Mutation Screening and Histochemical Analyses of Muscles from Patients

We performed *MYOT* mutation screening in MFM patients and identified two patients with mutations. Patient 1, harboring a *MYOT* c.179C→G (p.S60C) mutation in exon 2, was a 63-year-old woman with a 6-year-long history of slowly progressive limb muscle weakness. Her mother (deceased) had had muscle weakness. The patient had difficulty in climbing stairs without support, and could not walk for long distances. Her serum creatine kinase level was elevated to 734 IU/L (reference, <200 IU/L). A biopsied specimen from the rectus femoris muscle showed marked variation in fiber size, with some necrotic fibers. Clusters of degenerated fibers with abnormal cytoplasmic inclusions were observed; some fibers with rimmed vacuoles were also seen (Figure 1B). Intermyofibrillar networks were markedly disorganized (Figure 1D). Under electron microscopy, electron-dense materials and cytoplasmic amorphous inclusions of various sizes were seen in some fibers (see Supplemental Figure S1 at *http://ajp.amjpathol.org*). Patient 2 was a 57-year-old woman harboring a *MYOT* c.1214G→A (p.R405K) mutation in exon 9. Detailed clinical symptoms have been described previously.[23] In brief, this patient had a 16-year-long history of slowly progressive proximal limb muscle weakness. Her serum creatine kinase level was mildly elevated (385 IU/l). A specimen from the vastus lateralis muscle showed marked variation in fiber size, scattered fibers with internal nuclei, and small angular fibers. Some fibers with rimmed vacuoles were seen (Figure 1C), and intermyofibrillar networks were disorganized (Figure 1E). Immunohistochemical analysis of muscle specimens from both patients revealed scattered fibers with strong immunoreactive accumulations of myotilin (Figure 1, F and G), which costained with polyubiquitin (Figure 1, H and I), α-B crystallin, BAG3, actin, desmin, and filamin C (see Supplemental Figure S2 at *http://ajp.amjpathol.org*).

Mutant Myotilin Does Not Aggregate in Cultured Cells

To examine the aggregation of mutant myotilins in cultured cells, C2C12 murine myoblasts were transfected with Myc-tagged wtMYOT (Myc-wtMYOT) or Myc-tagged mMYOT (Myc-mMYOT S60C or R405K). After 48 hours, immunostaining with anti-Myc antibody and rhodamine-labeled phalloidin revealed that the expressed Myc-wtMYOT, Myc-mMYOT S60C, and Myc-mMYOT R405K did not form abnormal protein aggregations, and they localized at actin stress fibers (Figure 2). Expression of mMYOT did not affect differentiation of C2C12 cells (data not shown).

Accumulation of Myotilin after Electroporation

To investigate the roles of mutant myotilin, we performed *in vivo* electroporation to express Myc-wtMYOT or Myc-mMYOT (S60C or R405K) in mouse TA muscles. At 7 and 14 days after electroporation, Myc-positive granules with diameters >1 μm were observed in Myc-tagged myotilin-expressing myofibers (Figure 3A). Compared with wtMYOT-expressing myofibers, mMYOT-expressing myofi-

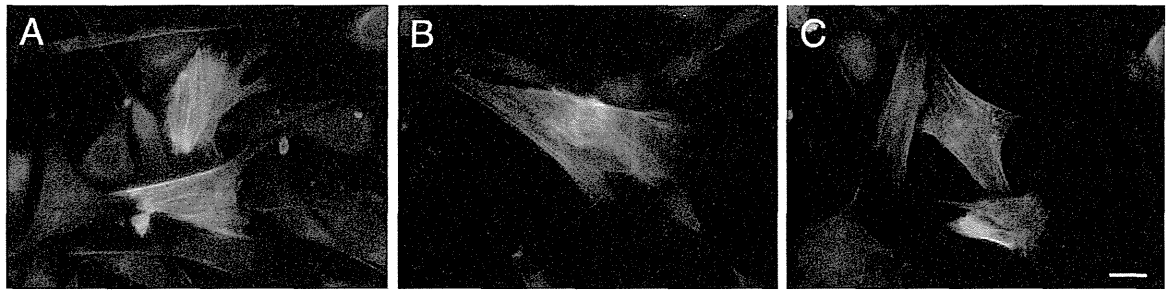

Figure 2. Expression of mutant myotilin in cultured cells. Immunofluorescence staining of transfected Myc-wtMYOT (**A**), Myc-mMYOT S60C (**B**), and Myc-mMYOT R405K (**C**) in C2C12 murine myoblasts. Merged images of Myc-tagged myotilin-expressing cells (green) costained for actin stress fibers (red), and nuclear staining with DAPI (blue). C2C12 myoblasts expressing mMYOT S60C (**B**) or R405K (**C**) did not exhibit protein aggregates, and the mutant myotilin colocalized with actin stress fibers similar to wtMYOT (**A**). Scale bar = 20 μm.

bers contained more granular aggregates that were larger in size. At 7 days after electroporation, Myc-positive aggregates of wtMYOT, mMYOT S60C, and mMYOT R405K were observed in 14 ± 5%, 44 ± 7%, and 21 ± 4% of muscle fibers, respectively (Figure 3B). At 14 days after electroporation, the number of the fibers with aggregates increased to 22 ± 4% in wtMYOT, 50 ± 2% in mMYOT S60C, and 37 ± 3% in mMYOT R405K (Figure 3C). The number and size of Myc-positive aggregates in 30 randomly selected Myc-positive muscle fibers were much higher in mMYOT S60C and slightly higher in mMYOT R405K at 14 days after electroporation than at 7 days (see Supplemental Figure S3 at *http://ajp.amjpathol.org*). These data indicate that the expressed mutant myotilins, and mMYOT S60C in particular, are prone to aggregate in skeletal muscles. The amounts of expressed Myc-tagged myotilin proteins were approximately equal, as measured by immunoblotting (Figure 3D).

Myofibril Disorganization and Z-Disk Streaming in Muscles Expressing Mutant Myotilins

To investigate the ultrastructural characteristics of mutant myotilin-electroporated muscles, we performed electron microscopy at 7 and 14 days after electroporation. In Toluidine Blue-stained longitudinal semithin sections, partial disorganization of the Z-disk was observed in both mMYOT S60C-expressing and mMYOT R405K-expressing TA muscles, but not in control or wtMYOT electroporated muscles (data not shown). Electron microscopy also revealed myofibril disorganization with disrupted Z-disk, such as Z-disk streaming and broadening, in mMYOT-expressing muscles (Figure 4, A and D). Variable-sized (1 to 8 μm in diameter) electron-dense material, with electron densities similar to that of the Z-disk, were also seen in mMYOT-expressing mouse muscles (Figure 4, B and E). The inclusions were occasionally associated with autophagic vacuoles (Figure 4, C and F). These ultrastructural findings were commonly observed in both mMYOT S60C- and mMYOT R405K-expressing mouse muscles.

Mutant Myotilin Aggregates Colocalize with Polyubiquitin and Other Z-Disk–Associated Proteins

To compare the protein accumulations in human and mouse muscles, we performed immunohistochemical analysis. At 14 days after electroporation, some cytoplasmic inclusions were observed in mGT-stained sections of mMYOT-expressing muscles (Figure 5, A and B). Immunostaining of serial sections revealed that the inclusions were immunopositive for the Myc tag (Figure 5, A and B). The aggregates of Myc-mMYOT (S60C and R405K) strongly colocalized with polyubiquitin and αB-crystallin. Accumulations of other Z-disk–associated proteins were also observed, including BAG3, actin, desmin, and filamin C (Figure 5). These findings are similar to the observations made in the patients' muscles (Figure 1, F–I; see also Supplemental Figure S2 at *http://ajp.amjpathol.org*). In the electroporated muscles, Myc-wtMYOT aggregates also colocalized with Z-disk–associated proteins, including αB-crystallin, BAG3, actin, desmin, and filamin C (data not shown), whereas only few wtMYOT aggregates were immunopositive for polyubiquitin (Figure 6A).

Mutant Myotilin Proteins Display Marked Detergent Insolubility with Polyubiquitinated Proteins

In the muscle specimens of the two myotilinopathy patients, myotilin aggregates exhibited positive staining for polyubiquitin (Figure 1; see also Supplemental Figure S3 at *http://ajp.amjpathol.org*). Similarly, in electroporated mouse muscles, mMYOT aggregates were positive for polyubiquitin, and polyubiquitin-positive aggregates were more prominently observed in mMYOT S60C-expressing muscles at 14 days after electroporation. On the other hand, only few aggregates of Myc-wtMYOT were positive for polyubiquitin (Figure 6A). This result suggests that mutant myotilin was ubiquitinated or that the expressed mutant myotilin induced the deposition of polyubiquitinated proteins in the muscles of patients and electroporated mice. To characterize these aggregates, we performed a solubility assay. The muscle

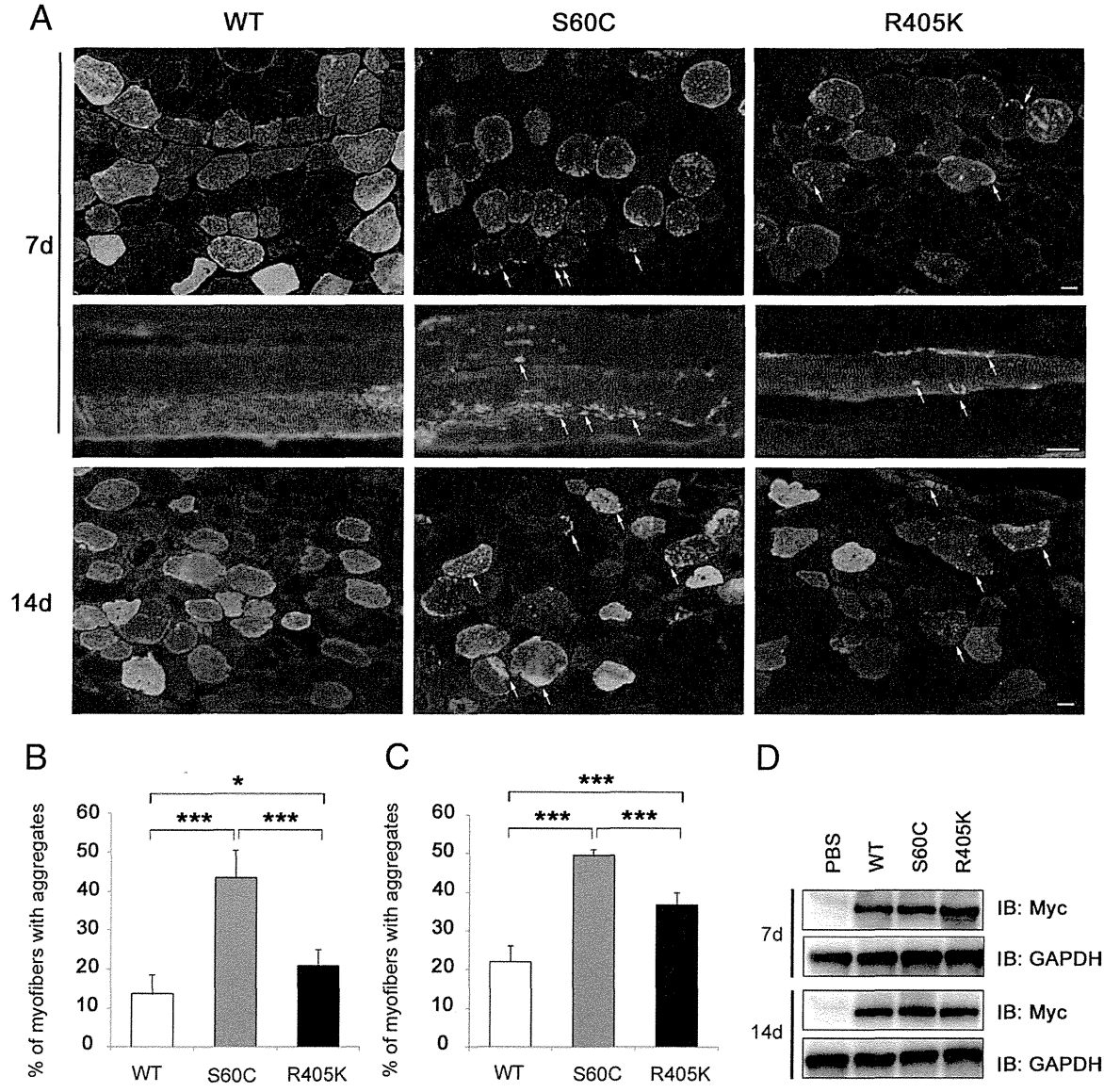

Figure 3. Enhanced aggregation of mutant myotilins in mouse skeletal muscle. **A:** Immunohistochemical staining of Myc-wtMYOT (WT)-electroporated or Myc-mMYOT (S60C or R405K)-electroporated mouse TA muscles. At 7 and 14 days after electroporation, S60C and R405K formed many Myc-positive granular aggregates (**arrows**) in myofibers, compared with WT. More prominent protein aggregates were observed in the S60C-electroporated muscle. At 14 days after electroporation, S60C-expressing myofibers exhibited larger aggregates. Scale bars: 20 μm. **B** and **C:** The percentage of myofibers with Myc-positive aggregates in the electroporated fibers of the WT, S60C, and R405K expression groups (n = 5 mice per group). $^{*}P < 0.05$; $^{***}P < 0.001$. **D:** Immunoblotting analysis of transfected Myc-tagged myotilin in 15 serial sections taken after the sections used for immunohistochemistry. GAPDH was used as a loading control.

specimen with the S60C mutation (patient 1) exhibited increased amounts of myotilin in the detergent-insoluble fraction, compared with the control specimens (Figure 6, B and D). Increasing amounts of polyubiquitinated proteins and αB-crystallin were also detected in the insoluble fraction. On the other hand, the solubilities of myotilin and other proteins, including polyubiquitin, in the muscle specimen with the R405K mutation (patient 2) were similar to those of controls (Figure 6B). Consistently, in the mouse muscles isolated at 14 days after electroporation, markedly increasing amounts of insoluble mMYOT S60C were observed (Figure 6C). In the PBS-injected control muscle, insolubility of endogenous myotilin was 31 ± 12%, whereas in the wtMYOT-, mMYOT S60C-, and mMYOT R405K-injected muscles, the Myc-tagged myotilin amounts in the insoluble fraction were 34 ± 10%, 69 ± 5%, and 48 ± 9%, respectively (Figure 6E). Insolubility of Myc-wtMYOT was similar to that of endogenous myotilin, but mMYOT, and S60C in particular, exhibited higher insolubility (Figure 6E).

These results are consistent with the number of intracellular aggregates observed after electroporation. The amount of polyubiquitinated proteins was markedly increased in the insoluble fraction of mMYOT S60C-electroporated muscles, similar to that of the muscle with the S60C mutation (patient 1) (Figure 6, B and C). A slight increase in the amount of detergent-insoluble polyubiquitinated proteins was observed in mMYOT R405K-electroporated muscles (Figure 6C). The amounts of other

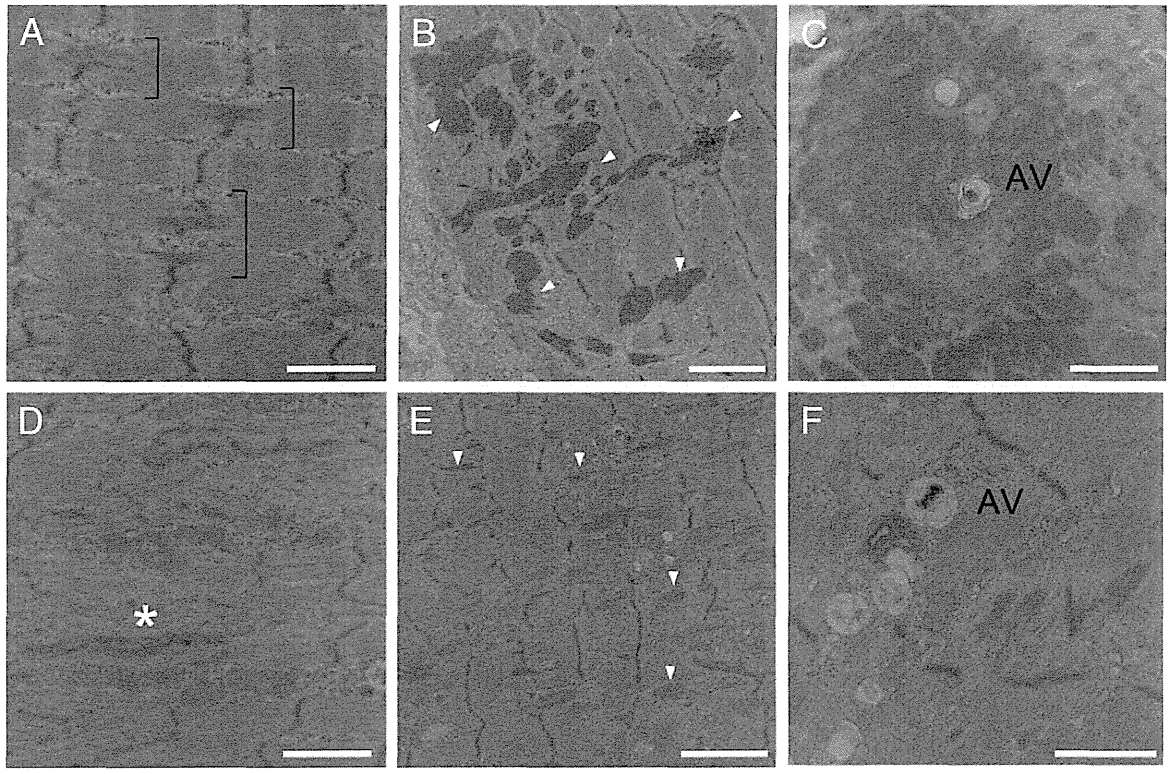

Figure 4. Electron microscopy of muscles expressing mutant myotilin. mMYOT S60C (**A–C**); mMYOT R405K (**D–F**). **A** and **D:** mMYOT-transfected muscle fibers exhibited myofibril disorganization with disrupted Z-disk; note broadening of Z-disks (**A**, **brackets**) and Z-disk streaming (**D**, **asterisk**). **B** and **E:** Variable-sized (1 to 8 μm in diameter) electron-dense inclusions (**arrowheads**) were seen in mMYOT-expressing muscles. **C** and **F:** Inclusions were occasionally associated with autophagic vacuoles (AV). **B** and **C:** Seven days after electroporation. **A** and **D–F:** Fourteen days after electroporation. Scale bars: 3.0 μm (**B** and **E**); 2.0 μm (**C**); 1.7 μm (**A** and **D**); 1.4 μm (**F**).

Z-disk–associated proteins, including αB-crystallin, in the insoluble fraction did not exhibit an increase, even in mMYOT S60C-electroporated muscles (Figure 6C; see also Supplemental Figure S4, A and B, at *http://ajp.amjpathol.org*). We also performed an immunoprecipitation assay to examine whether myotilin was polyubiquitinated. Myc-tagged myotilin proteins were immunoprecipitated from the detergent-soluble fraction of the mouse muscles isolated at 14 days after electroporation. Polyubiquitin immunoreactivity was not detected in the immunoprecipitated proteins (see Supplemental Figure S4C at *http://ajp.amjpathol.org*), indicating that neither the wt-MYOT nor the mMYOT proteins in the soluble fraction were polyubiquitinated.

Discussion

Patients with MFM, including myotilinopathy, exhibit variable clinical features. Some patients exhibit progressive weakness in proximal muscles, whereas others exhibit distal dominant muscle involvement. Cardiomyopathy, peripheral neuropathy, and respiratory insufficiency may be observed.[2] The diagnosis of MFM is generically based on characteristic pathological findings in biopsied muscles, namely, myofibrillar degradation and protein aggregation.[1] Histochemically, the most remarkable pathological changes were observed with mGT staining (Figure 1). Abnormal protein aggregates were observed, including amorphous, granular, or hyaline deposits of various sizes, shapes, and colors (dark blue, blue red, or dark green). The presence of rimmed and nonrimmed vacuoles was also a characteristic observation. Furthermore, NADH-TR staining revealed intermyofibrillar network disorganization. Attenuation or absence of NADH-TR activity in focal areas of myofibers is also observed in MFM.[1,31]

Here, we have presented findings for myotilinopathy patients with similar clinical features but different pathological changes. Fibers with cytoplasmic inclusions and disorganized myofibrils were prominent in the patient with S60C mutation, and these inclusions were strongly immunoreactive for myotilin (Figure 1).

Although transfected cultured cells did not show aggregations, our *in vivo* expression studies in mice were able to reproduce the pathological changes observed in myotilinopathy patients. Mutant myotilin caused enhanced protein aggregation in TA muscles within 1 to 2 weeks (Figure 3). The dark blue or dark green inclusions stained by mGT in mutant-expressing fibers (Figure 4) were similar to those observed in the myotilinopathy patients. Furthermore, mMYOT S60C-expressing myofibers exhibited a greater number of aggregates, which is consistent with the pathology of the patient with that mutation (patient 1). Of note, the size of mMYOT S60C aggregates markedly increased over time, suggesting that mutant myotilin may be resistant to protein degra-

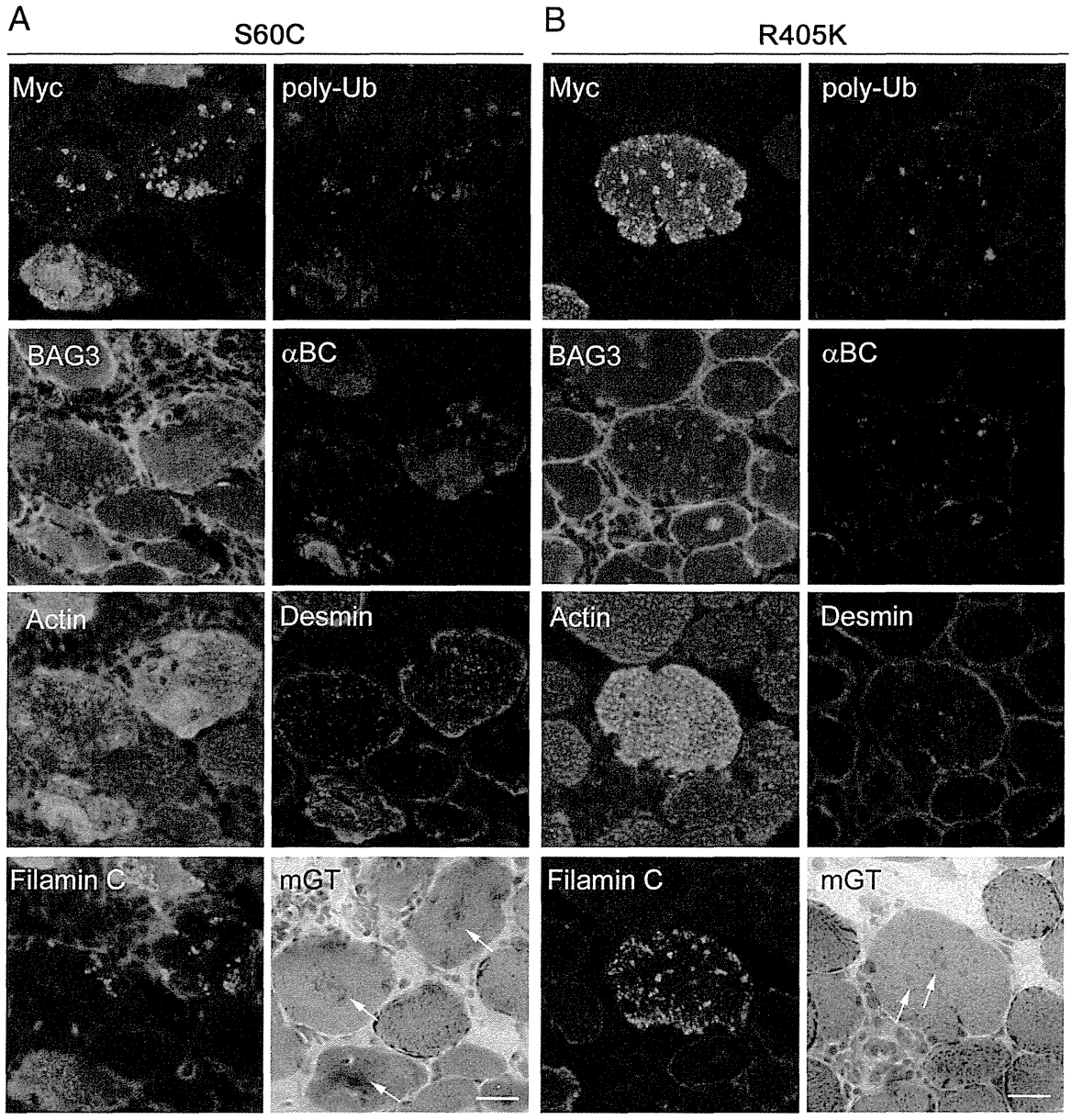

Figure 5. Mutant myotilin aggregates colocalize with polyubiquitin and other Z-disk–associated proteins in electroporated mouse muscle. mGT and immunohistochemical staining of mouse muscle expressing Myc-mMYOT S60C (**A**) or mMYOT R405K (**B**) at 14 days after electroporation. On mGT-stained sections of mMYOT-expressing muscles, cytoplasmic inclusions (**arrows**) were seen. The inclusions were immunopositive for the Myc tag in serial sections. The Myc-positive aggregates of S60C and R405K strongly colocalized with polyubiquitin (poly-Ub) and αB-crystallin (αBC). The aggregates were also immunopositive for BAG3, actin, desmin, and filamin C. Scale bars: 20 μm (**A** and **B**).

dation, as described previously for MFM-associated mutant desmin.[32,33]

Focal disorganization of myofibrils, Z-disk streaming, and accumulation of electron-dense material near the Z-disk are characteristic electron microscopic findings in the muscles of MFM patients.[17,34,35] In the myotilinopathy patient, Z-disk streaming, numerous autophagic vacuoles[17] and cytoplasmic amorphous inclusions were observed (see Supplemental Figure S2 at *http://ajp.amjpathol.org*). In the present study, expression of mMYOT by electroporation elicited myofibril disorganization and accumulation of electron-dense material, which are ultrastructural hallmarks of MFM (Figure 5). Autophagic vacuoles associated with inclusions were also observed in electroporated muscles. Disorganization of myofibrils starting from the Z-disk and material appearing to originate from the Z-disk are commonly observed in MFM patients,[34,35] and these features were also observed in the mMYOT-electroporated muscles. These morphological findings imply that the presence of mutant myotilin can induce characteristic pathological features by affecting Z-disk structure.

Ectopic accumulations of multiple proteins, including Z-disk–associated proteins, are typical pathological features of MFM.[36,37] This study and previous reports[23,38] showed that myotilin-positive protein aggregates colocal-

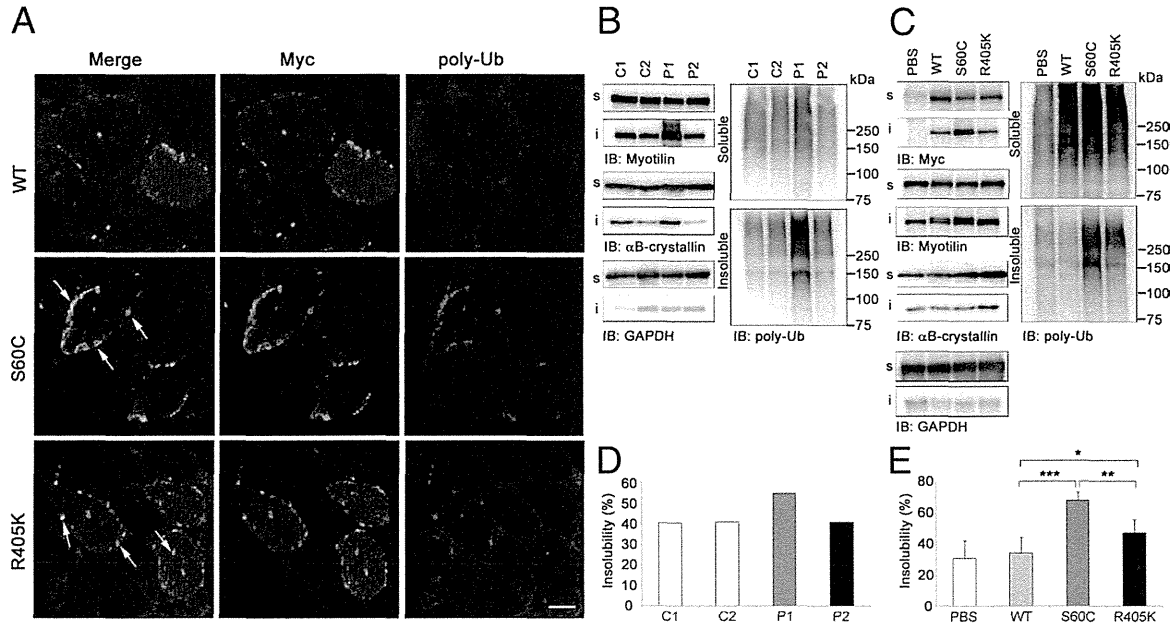

Figure 6. Mutant myotilin displays marked detergent insolubility, along with polyubiquitinated proteins. **A:** At 14 days after electroporation of Myc-wtMYOT (WT) or Myc-mMYOT (S60C or R405K), Myc-mMYOT aggregates, particularly those of S60C, colocalized with polyubiquitin (polyUb) (**arrows**). The WT aggregates rarely costained with polyubiquitin. **B–E** Solubilities of myotilin, polyubiquitinated proteins, and other sarcomeric proteins in muscles from myotilinopathy patients (**B** and **D**) and from electroporated mice (**C** and **E**). GAPDH was used as a loading control. **B:** Immunoblotting of detergent-soluble and detergent-insoluble fractions of muscles from control subjects (C1 and C2) or myotilinopathy patients [P1 (patient 1) and P2 (patient 2)]. In the muscles from P1 with S60C, markedly increasing amounts of myotilin, polyubiquitinated proteins, and αB-crystallin were detected in the insoluble fraction, compared with muscles from control subjects. **D:** Quantification of myotilin insolubilities revealed highest insolubility in P1. **C:** Immunoblotting of detergent-soluble and detergent-insoluble fractions of WT, S60C, or R405K-expressing muscles at 14 days after electroporation. Increasing amounts of insoluble Myc-tagged myotilin proteins and polyubiquitinated proteins were observed in mMYOT-electroporated muscles, compared with WT. Particularly in S60C-electroporated muscles, the amounts of insoluble proteins were notably increased. **E:** Quantification of the insolubilities of electroporated Myc-tagged myotilin in the WT, S60C, and R405K expression groups (n = 6 mice per group). Insolubility of endogenous myotilin was measured using PBS-treated mouse muscles. Compared with WT, insolubilities of electroporated Myc-tagged myotilin were significantly increased in S60C and R405K. $^{*}P < 0.05$; $^{**}P < 0.01$; $^{***}P < 0.001$. Scale bar = 20 μm.

ize with ubiquitin and Z-disk–associated proteins (ie, αB-crystallin, BAG3, actin, desmin, and filamin C) in the muscles of myotilinopathy patients (Figure 1; see also Supplemental Figure S2 at *http://ajp.amjpathol.org*). It has been reported that the myotilin T57I transgenic mice develop progressive myofibrillar changes, including Z-disk streaming and accumulation of mutant myotilin with ubiquitin and Z-disk–associated proteins, similar to those observed in myotilinopathy patients.[28] Expression of mMYOT elicited similar cytoplasmic aggregations in mouse skeletal muscle, and within 2 weeks the aggregates colocalized with polyubiquitin and other Z-disk–associated proteins. Our results indicate that mutant myotilin is able to nucleate aggregations of Z-disk–associated proteins in skeletal muscle.

MFM is a proteinopathy (ie, a protein accumulation disease). In these diseases, protein aggregates are operationally defined by poor solubility in aqueous or detergent solvents.[39,40] Such insoluble protein aggregations are characteristic of many neurodegenerative diseases.[41] In the present study, we discovered that the mutant myotilin S60C protein, along with polyubiquitinated proteins, exhibited marked detergent insolubility in muscles from both the patient and electroporated mice. Mutant myotilin R405K protein showed increased, but lower, detergent insolubility in mice (Figure 6), which may be consistent with the observation that the muscle from the patient with the R405K mutation exhibited only mild protein aggregation (Figure 1). The different detergent insolubilities exhibited by the two *MYOT* mutations may closely correlate with the amounts of protein aggregation. Here, we confirmed the aggregation-prone property of mutant myotilin, which participates in the pathogenesis of myotilinopathy. Using an immunoprecipitation assay, we also showed that electroporated mMYOT was not ubiquitinated in the detergent-soluble fraction (see Supplemental Figure S4 at *http://ajp.amjpathol.org*). A previous study showed that transfected myotilin is degraded by the proteasome system in cultured cells.[42] Our present findings show that ubiquitinated mutant myotilin can form insoluble aggregates. It is also possible that aggregation of insoluble ubiquitinated proteins is induced by the expression of mutant myotilin.

Several causative genes have been identified for MFM; however, in previous studies no mutations were found in nearly half of the MFM patients.[2] To identify the unknown causative genes, easy methods are required for determining the pathogenicity of novel mutations. Some mutant proteins exhibit protein aggregation[43–45] or biological dysfunction, including protein-protein interaction *in vitro*.[23,46–48] However, we could not detect any protein aggregation in mMYOT-expressing cultured cells (Figure 2). The difficulty of *in vitro* investigation may be responsible for the inability to identify Z-disk–associated proteins or mature Z-disk structures. Indeed, myotilin is expressed in later differentiated C2C12 myotubes with

sarcomere-like structures.[49] This suggests that mutant myotilin requires mature Z-disk and/or other sarcomeric proteins to cause aggregations. In such cases, *in vivo* examination is important for evaluating the pathogenicity of mutations. Because *in vivo* electroporation can reproduce the pathological changes observed in MFM patients within a short time, it is a useful and powerful tool for evaluating the pathogenicity of mutations in MFM.

Acknowledgments

We thank Dr. Alan H. Beggs (Children's Hospital Boston, Harvard Medical School) for the kind gift of anti-filamin C antibody and Dr. Satomi Mitsuhashi (Children's Hospital Boston, Harvard Medical School) for technical assistance in electron microscopy analysis.

References

1. Selcen D: Myofibrillar myopathies. Neuromuscul Disord 2011, 21: 161–171
2. Selcen D, Engel AG: Myofibrillar myopathy. (Updated) In GeneReviews. Copyright University of Washington, Seattle. 1997–2012. Available at http://www.ncbi.nlm.nih.gov/books/NBK1499, last revised July 27, 2010
3. OlivÉ M, Odgerel Z, Martínez A, Poza JJ, Bragado FG, Zabalza RJ, Jericó I, Gonzalez-Mera L, Shatunov A, Lee HS, Armstrong J, Maraví E, Arroyo MR, Pascual-Calvet J, Navarro C, Paradas C, Huerta M, Marquez F, Rivas EG, Pou A, Ferrer I, Goldfarb LG: Clinical and myopathological evaluation of early- and late-onset subtypes of myofibrillar myopathy. Neuromuscul Disord 2011, 21:533–542
4. Salmikangas P, Mykkänen OM, Grönholm M, Heiska L, Kere J, Carpén O: Myotilin, a novel sarcomeric protein with two Ig-like domains, is encoded by a candidate gene for limb-girdle muscular dystrophy. Hum Mol Genet 1999, 8:1329–1336
5. Parast MM, Otey CA: Characterization of palladin, a novel protein localized to stress fibers and cell adhesions. J Cell Biol 2000, 150: 643–656
6. Mykkänen OM, Grönholm M, Rönty M, Lalowski M, Salmikangas P, Suila H, Carpén O: Characterization of human palladin, a microfilament-associated protein. Mol Biol Cell 2001, 12:3060–3073
7. Bang ML, Mudry RE, McElhinny AS, Trombitas K, Geach AJ, Yamasaki R, Sorimachi H, Granzier H, Gregorio CC, Labeit S: Myopalladin, a novel 145-kilodalton sarcomeric protein with multiple roles in Z-disc and I-band protein assemblies. J Cell Biol 2001, 153:413–427
8. Faulkner G, Lanfranchi G, Valle G: Telethonin and other new proteins of the Z-disc of skeletal muscle. IUBMB Life 2001, 51:275–282
9. Frank D, Kuhn C, Katus HA, Frey N: The sarcomeric Z-disc: a nodal point in signalling and disease. J Mol Med (Berl) 2006, 84:446–468
10. van der Ven PF, Wiesner S, Salmikangas P, Auerbach D, Himmel M, Kempa S, Hayess K, Pacholsky D, Taivainen A, Schröder R, Carpén O, Fürst DO: Indications for a novel muscular dystrophy pathway. gamma-Filamin, the muscle-specific filamin isoform, interacts with myotilin. J Cell Biol 2000, 151:235–248
11. Gontier Y, Taivainen A, Fontao L, Sonnenberg A, van der Flier A, Carpen O, Faulkner G, Borradori L: The Z-disc proteins myotilin and FATZ-1 interact with each other and are connected to the sarcolemma via muscle-specific filamins. J Cell Sci 2005, 118:3739–3749
12. von Nandelstadh P, Ismail M, Gardin C, Suila H, Zara I, Belgrano A, Valle G, Carpen O, Faulkner G: A class III PDZ binding motif in the myotilin and FATZ families binds enigma family proteins: a common link for Z-disc myopathies. Mol Cell Biol 2009, 29:822–834
13. Witt SH, Granzier H, Witt CC, Labeit S: MURF-1 and MURF-2 target a specific subset of myofibrillar proteins redundantly: towards understanding MURF-dependent muscle ubiquitination. J Mol Biol 2005, 350:713–722
14. Salmikangas P, van der Ven PF, Lalowski M, Taivainen A, Zhao F, Suila H, Schröder R, Lappalainen P, Fürst DO, Carpén O: Myotilin, the limb-girdle muscular dystrophy 1A (LGMD1A) protein, cross-links actin filaments and controls sarcomere assembly. Hum Mol Genet 2003, 12:189–203
15. von Nandelstadh P, Grönholm M, Moza M, Lamberg A, Savilahti H, Carpén O: Actin-organising properties of the muscular dystrophy protein myotilin. Exp Cell Res 2005, 310:131–139
16. Selcen D: Myofibrillar myopathies. Curr Opin Neurol 2008, 21:585–589
17. Olivé M, Goldfarb LG, Shatunov A, Fischer D, Ferrer I: Myotilinopathy: refining the clinical and myopathological phenotype. Brain 2005, 128:2315–2326
18. Foroud T, Pankratz N, Batchman AP, Pauciulo MW, Vidal R, Miravalle L, Goebel HH, Cushman LJ, Azzarelli B, Horak H, Farlow M, Nichols WC: A mutation in myotilin causes spheroid body myopathy. Neurology 2005, 65:1936–1940
19. Hauser MA, Conde CB, Kowaljow V, Zeppa G, Taratuto AL, Torian UM, Vance J, Pericak-Vance MA, Speer MC, Rosa AL: Myotilin mutation found in second pedigree with LGMD1A. Am J Hum Genet 2002, 71:1428–1432
20. Hauser MA, Horrigan SK, Salmikangas P, Torian UM, Viles KD, Dancel R, Tim RW, Taivainen A, Bartoloni L, Gilchrist JM, Stajich JM, Gaskell PC, Gilbert JR, Vance JM, Pericak-Vance MA, Carpen O, Westbrook CA, Speer MC: Myotilin is mutated in limb girdle muscular dystrophy 1A. Hum Mol Genet 2000, 9:2141–2147
21. Penisson-Besnier I, Talvinen K, Dumez C, Vihola A, Dubas F, Fardeau M, Hackman P, Carpen O, Udd B: Myotilinopathy in a family with late onset myopathy. Neuromuscul Disord 2006, 16:427–431
22. Berciano J, Gallardo E, Dominguez-Perles R, Garcia A, Garcia-Barredo R, Combarros O, Infante J, Illa I: Autosomal-dominant distal myopathy with a myotilin S55F mutation: sorting out the phenotype. J Neurol Neurosurg Psychiatry 2008, 79:205–208
23. Shalaby S, Mitsuhashi H, Matsuda C, Minami N, Noguchi S, Nonaka I, Nishino I, Hayashi YK: Defective myotilin homodimerization caused by a novel mutation in MYOT exon 9 in the first Japanese limb girdle muscular dystrophy 1A patient. J Neuropathol Exp Neurol 2009, 68:701–707
24. Reilich P, Krause S, Schramm N, Klutzny U, Bulst S, Zehetmayer B, Schneiderat P, Walter MC, Schoser B, Lochmüller H: A novel mutation in the myotilin gene (MYOT) causes a severe form of limb girdle muscular dystrophy 1A (LGMD1A). J Neurol 2011, 258:1437–1444
25. Mavroidis M, Panagopoulou P, Kostavasili I, Weisleder N, Capetanaki Y: A missense mutation in desmin tail domain linked to human dilated cardiomyopathy promotes cleavage of the head domain and abolishes its Z-disc localization. FASEB J 2008, 22:3318–3327
26. Wang X, Osinska H, Klevitsky R, Gerdes AM, Nieman M, Lorenz J, Hewett T, Robbins J: Expression of R120G-alphaB-crystallin causes aberrant desmin and alphaB-crystallin aggregation and cardiomyopathy in mice. Circ Res 2001, 89:84–91
27. Wang X, Osinska H, Dorn GW 2nd, Nieman M, Lorenz JN, Gerdes AM, Witt S, Kimball T, Gulick J, Robbins J: Mouse model of desmin-related cardiomyopathy. Circulation 2001, 103:2402–2407
28. Garvey SM, Miller SE, Claflin DR, Faulkner JA, Hauser MA: Transgenic mice expressing the myotilin T57I mutation unite the pathology associated with LGMD1A and MFM. Hum Mol Genet 2006, 15:2348–2362
29. Hayashi YK, Matsuda C, Ogawa M, Goto K, Tominaga K, Mitsuhashi S, Park YE, Nonaka I, Hino-Fukuyo N, Haginoya K, Sugano H, Nishino I: Human PTRF mutations cause secondary deficiency of caveolins resulting in muscular dystrophy with generalized lipodystrophy. J Clin Invest 2009, 119:2623–2633
30. Thompson TG, Chan YM, Hack AA, Brosius M, Rajala M, Lidov HG, McNally EM, Watkins S, Kunkel LM: Filamin 2 (FLN2): A muscle-specific sarcoglycan interacting protein. J Cell Biol 2000, 148:115–126
31. Schröder R, Schoser B: Myofibrillar myopathies: a clinical and myopathological guide. Brain Pathol 2009, 19:483–492
32. Liu J, Chen Q, Huang W, Horak KM, Zheng H, Mestril R, Wang X: Impairment of the ubiquitin-proteasome system in desminopathy mouse hearts. FASEB J 2006, 20:362–364
33. Liu J, Tang M, Mestril R, Wang X: Aberrant protein aggregation is essential for a mutant desmin to impair the proteolytic function of the ubiquitin-proteasome system in cardiomyocytes. J Mol Cell Cardiol 2006, 40:451–454
34. Selcen D, Ohno K, Engel AG: Myofibrillar myopathy: clinical, morphological and genetic studies in 63 patients. Brain 2004, 127:439–451

35. Claeys KG, Fardeau M, Schröder R, Suominen T, Tolksdorf K, Behin A, Dubourg O, Eymard B, Maisonobe T, Stojkovic T, Faulkner G, Richard P, Vicart P, Udd B, Voit T, Stoltenburg G: Electron microscopy in myofibrillar myopathies reveals clues to the mutated gene. Neuromuscul Disord 2008, 18:656–666
36. Claeys KG, van der Ven PF, Behin A, Stojkovic T, Eymard B, Dubourg O, Laforêt P, Faulkner G, Richard P, Vicart P, Romero NB, Stoltenburg G, Udd B, Fardeau M, Voit T, Fürst DO: Differential involvement of sarcomeric proteins in myofibrillar myopathies: a morphological and immunohistochemical study. Acta Neuropathol 2009, 117:293–307
37. Olivé M: Extralysosomal protein degradation in myofibrillar myopathies. Brain Pathol 2009, 19:507–515
38. Janué A, Olivé M, Ferrer I: Oxidative stress in desminopathies and myotilinopathies: a link between oxidative damage and abnormal protein aggregation. Brain Pathol 2007, 17:377–388
39. Fink AL: Protein aggregation: folding aggregates, inclusion bodies and amyloid. Fold Des 1998, 3:R9–R23
40. Kopito RR: Aggresomes, inclusion bodies and protein aggregation. Trends Cell Biol 2000, 10:524–530
41. Ross CA, Poirier MA: Protein aggregation and neurodegenerative disease. Nat Med 2004, 10:S10–S17
42. von Nandelstadh P, Soliymani R, Baumann M, Carpen O: Analysis of myotilin turnover provides mechanistic insight into the role of myotilinopathy-causing mutations. Biochem J 2011, 436:113–121
43. Goldfarb LG, Vicart P, Goebel HH, Dalakas MC: Desmin myopathy. Brain 2004, 127:723–734
44. Vicart P, Caron A, Guicheney P, Li Z, Prévost MC, Faure A, Chateau D, Chapon F, Tomé F, Dupret JM, Paulin D, Fardeau M: A missense mutation in the alphaB-crystallin chaperone gene causes a desmin-related myopathy. Nat Genet 1998, 20:92–95
45. Selcen D, Muntoni F, Burton BK, Pegoraro E, Sewry C, Bite AV, Engel AG: Mutation in BAG3 causes severe dominant childhood muscular dystrophy. Ann Neurol 2009, 65:83–89
46. Sharma S, Mücke N, Katus HA, Herrmann H, Bär H: Disease mutations in the "head" domain of the extra-sarcomeric protein desmin distinctly alter its assembly and network-forming properties. J Mol Med (Berl) 2009, 87:1207–1219
47. Bär H, Kostareva A, Sjöberg G, Sejersen T, Katus HA, Herrmann H: Forced expression of desmin and desmin mutants in cultured cells: impact of myopathic missense mutations in the central coiled-coil domain on network formation. Exp Cell Res 2006, 312:1554–1565
48. Bova MP, Yaron O, Huang Q, Ding L, Haley DA, Stewart PL, Horwitz J: Mutation R120G in alphaB-crystallin, which is linked to a desmin-related myopathy, results in an irregular structure and defective chaperone-like function. Proc Natl Acad Sci USA 1999, 96:6137–6142
49. Mologni L, Moza M, Lalowski MM, Carpén O: Characterization of mouse myotilin and its promoter. Biochem Biophys Res Commun 2005, 329:1001–1009

Available online at www.sciencedirect.com

SciVerse ScienceDirect

Neuromuscular Disorders 22 (2012) 389–393

www.elsevier.com/locate/nmd

Case report

Acid phosphatase-positive globular inclusions is a good diagnostic marker for two patients with adult-onset Pompe disease lacking disease specific pathology

Rie S. Tsuburaya [a,b], Kazunari Monma [a], Yasushi Oya [a], Takahiro Nakayama [c], Tokiko Fukuda [d], Hideo Sugie [d], Yukiko K. Hayashi [a], Ikuya Nonaka [a], Ichizo Nishino [a,*]

[a] *Department of Neuromuscular Research, National Institute of Neuroscience, National Center of Neurology and Psychiatry, Kodaira, Tokyo, Japan*
[b] *Department of Pediatrics, Tohoku University School of Medicine, Miyagi, Japan*
[c] *Department of Neurology, Yokohama Rosai Hospital, Kanagawa, Japan*
[d] *Department of Pediatrics, Jichi Medical University and Jichi Children's Medical Center, Tochigi, Japan*

Received 18 August 2011; received in revised form 19 October 2011; accepted 15 November 2011

Abstract

Diagnosis of adult-onset Pompe disease is sometimes challenging because of its clinical similarities to muscular dystrophy and the paucity of disease-specific vacuolated fibers in the skeletal muscle pathology. We describe two patients with adult-onset Pompe disease whose muscle pathology showed no typical vacuolated fibers but did show unique globular inclusions with acid phosphatase activity. The acid phosphatase-positive globular inclusions may be a useful diagnostic marker for adult-onset Pompe disease even when typical vacuolated fibers are absent.

Keywords: Pompe disease; *GAA*; Globular inclusion; Acid phosphatase

1. Introduction

Pompe disease (glycogen storage disease type 2; acid maltase deficiency; OMIM #232300) is an autosomal recessive disease caused by mutations in the gene encoding acid α-glucosidase (GAA, OMIM #606800), a lysosomal enzyme involved in glycogen degradation [1]. Based on age of onset and clinical severity, which depends on residual GAA activity, the disease can be classified into infantile, childhood-onset, and adult-onset forms.

Most of the infantile and childhood-onset forms exhibit disease-specific skeletal muscle pathology, which shows fibers occupied by huge vacuoles that contain basophilic amorphous materials. However, diagnosis of the adult-onset form is sometimes challenging due to clinical similarities to muscular dystrophy and the paucity of typical vacuolated myofibers. We diagnosed 37 patients with Pompe disease including 11 infantile, 16 childhood-onset, and 10 adult-onset forms in the muscle repository of the National Center of Neurology and Psychiatry (NCNP), Japan, based on a deficiency of GAA enzyme activity assayed using biopsied muscles, as previously described [2]. Among these 37 patients, two unrelated Japanese patients did not have disease-specific vacuolated muscle fibers but did have unique cytoplasmic inclusions. Here, we report the diagnostic utility of acid phosphatase (ACP)-positive globular inclusions for adult-onset Pompe disease.

* Corresponding author. Address: National Institute of Neuroscience, National Center of Neurology and Psychiatry, 4-1-1 Ogawahigashi-cho, Kodaira, Tokyo 187-8502, Japan. Tel.: +81 42 341 2711; fax: +81 42 346 1742.
E-mail address: nishino@ncnp.go.jp (I. Nishino).

0960-8966/$ - see front matter © 2011 Elsevier B.V. All rights reserved.
doi:10.1016/j.nmd.2011.11.003

2. Case report

2.1. Clinical summary

Patient 1: A 44-year-old man had been well until the age of 41 years when he started having difficulty in running. He was admitted to the hospital because of progressive muscle weakness. His parents were first cousins, but there was no family history of neuromuscular disorders. He was clinically suspected to suffer from muscular dystrophy because of slowly progressive muscle weakness and elevated creatine kinase levels of around 800 IU/L (normal, <171 IU/L). On examination, he had grade 4-muscle weakness on medical research council (MRC) scale and marked atrophy in his thighs. He did not have apparent respiratory impairment. Electromyography (EMG) showed myopathic changes with fibrillation and increased polyphasic motor unit potentials (MUPs).

Patient 2: A 62-year-old woman first noticed difficulty in climbing stairs at the age of 35 years, and needed a stick to walk at 45 years. Muscle weakness gradually worsened predominantly in her proximal limbs, and she became wheelchair-bound at 55 years. A muscle biopsy was performed at the age of 61 years. On examination, she had muscle weakness and atrophy predominantly in the proximal upper and lower limbs at the grade 3–4 on MRC scale. Serum CK level was 70 IU/L (normal, <142 IU/L). An EMG showed myopathic changes with increased polyphasic MUPs and myotonic-like repetitive discharges. She had been on non-invasive positive-pressure ventilation since the age of 62 years when the respiratory insufficiency appeared.

2.2. Skeletal muscle pathology

The skeletal muscle pathology from the vastus lateralis of patient 1 and from the biceps brachi of patient 2 showed nonspecific myopathic changes with moderate fiber size variation, mild endomysial fibrosis, and some fiber splitting (Fig. 1A). No necrotic or regenerating fibers were seen. No vacuoles containing amorphous materials were observed. Importantly, both muscles contained red–purple globular inclusions on modified Gomori-trichrome (mGT) stain (Fig. 1A and B). The average percentages of fibers with globular inclusions in the whole mGT-stained section were 0.5% in patient 1 and 2% in patient 2. These inclusions were invariably highlighted by ACP stain but not stained by periodic acid Schiff (PAS) (Fig. 1C). Inclusions were stained only faintly on menadione-linked α-glycerophosphate dehydrogenase (MAG) without substrate (Fig. 3A). Fibers with ACP-positive globular inclusions were also found in 15 of 16 childhood-onset and seven of eight adult-onset patients with disease-specific pathology in varying proportions (0.1–10%). The rate of fibers with inclusions was not significantly different between the childhood-onset and adult-onset forms. Fibers carrying inclusions did not have typical vacuoles with amorphous materials inside. In the infantile cases, more than 90% of the fibers were vacuolated, whereas non-vacuolated fibers with inclusions were hardly recognizable.

Double immunostaining was performed using primary antibodies against a lysosomal marker, lysosomal associated membrane protein-2 (LAMP-2; Developmental Studies Hybridoma Bank (DSHB), Iowa City, IA, USA) and an autophagosomal marker, microtubule-associated protein 1 light chain 3 (LC3; Novus Biologicals, Littleton, CO, USA). In fibers with ACP-positive inclusions, immunoreactivity for LAMP-2 and LC3 were accumulated focally in inclusions and surrounding area (Fig. 1D). We also examined another samples from adult-onset patients with typical vacuoles. Fibers with typical vacuoles were entirely positive for LAMP-2 and LC3 (data not shown).

On PAS staining, performed on epon-embedded sections (Epon-PAS) to detect glycogen more sensitively, PAS was negative in globular inclusions but positive in the surrounding area (Fig. 1E).

Electron micrography was performed as previously described using a Tecnai spirit transmission electron microscope (FEI, Hillsboro, OR, USA) [3]. The inclusions consisted of homogeneous electron-dense globules surrounded by increased glycogen particles and autophagic vacuoles (Fig. 1F). The globules contained neither dotted glycogen particles nor a filamentous structure.

2.3. GAA enzymatic analysis and genetic analysis

Presence of globular inclusions led us to suspect Pompe disease, and GAA enzymatic activity analyses revealed 7.5% of normal control activity in patient 1 and 12.3% in patient 2.

Genomic DNA was extracted from peripheral lymphocytes or biopsied muscle using a standard protocol for mutational analysis of *GAA*. All exons and their flanking intronic regions of *GAA* were amplified by PCR and directly sequenced with an ABI PRISM 3100 Automated Sequencer (Applied Biosystems, Foster City, CA, USA). Both patients carried the homozygous *GAA* mutation at the last codon of exon 2 (c. 546G > T). RT-PCR and direct sequencing were performed using RNA extracted from biopsied muscles. This novel mutation causes aberrant splicing by skipping exon 2 (Fig. 2). This homozygous c. 546G > T mutation was also found in another patient with the adult-onset form, whose muscle pathology showed typical skeletal muscle pathology with vacuolated fibers.

3. Discussion

ACP-positive globular inclusions were a good diagnostic marker for the two patients with adult-onset Pompe disease lacking typical vacuolated fibers. Among 12,103 muscle biopsies in the NCNP repository from 1979 to 2010, ACP-positive globular inclusions were not reported, except for Pompe disease.

The globular inclusions are most likely the same as "reducing body-like globular inclusions in late-onset Pompe disease" reported by Sharma et al., as the pathological features are

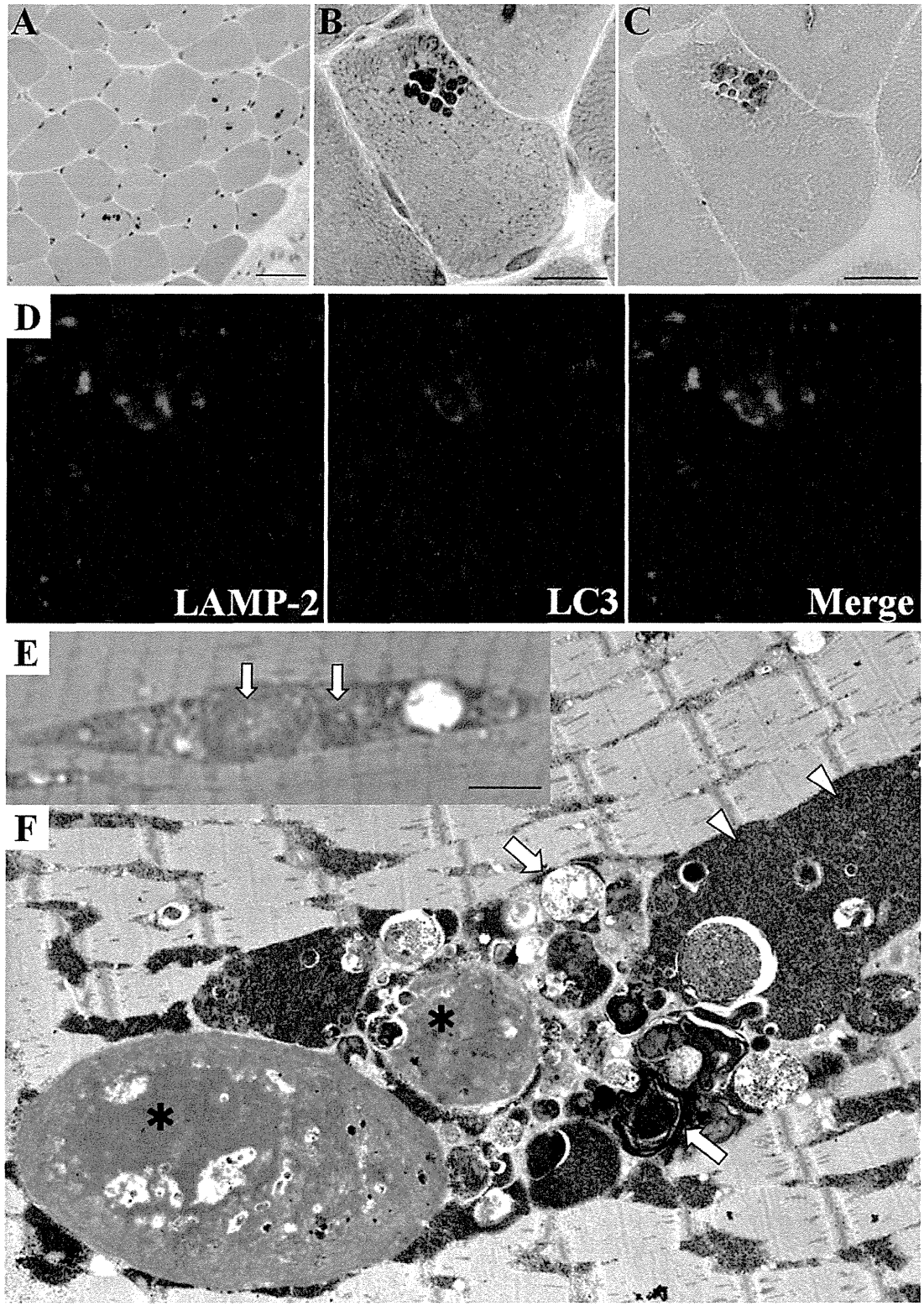

Fig. 1. Acid phosphatase-positive globular inclusions in patient 2. (A and B) Biopsied skeletal muscle showed nonspecific myopathic changes with scattered red–purple colored globular inclusions on modified Gomori-trichrome stain. (C) The inclusions have intense activity on acid phosphatase stain. Bar = 20 μm. (D) Double immunostaining for LAMP-2 (green) and LC3 (red) demonstrates colocalization of positive immunoreactions in the inclusions and surrounding area (B–D; serial sections). (E) On epon-embedded section, periodic acid Schiff stain is negative in inclusions (arrows). Bar = 5 μm. (F) On electron microscopy, globular inclusions (asterisks) lack Z-line structure, which differs from cytoplasmic bodies. Autophagic vacuoles (arrows) and glycogen particles (arrow heads) are seen in the vicinity of globular inclusions (12000×).

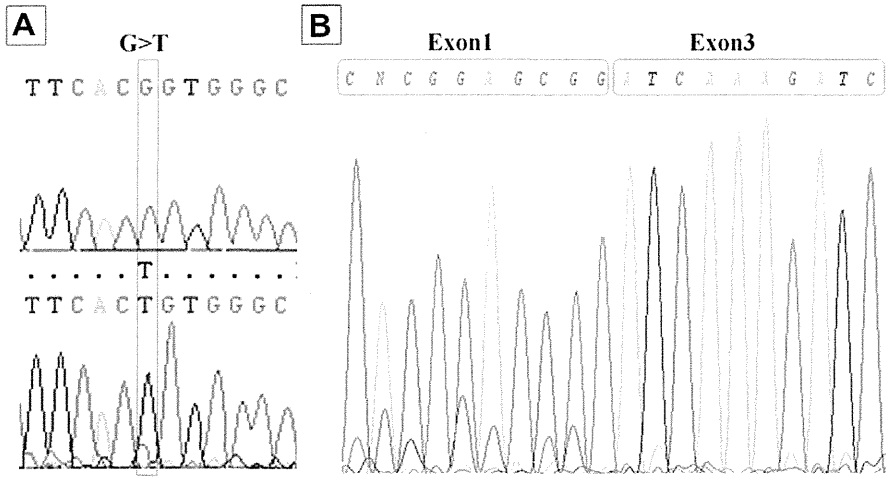

Fig. 2. Mutational analysis of *GAA*. Both patient have a homozygous c. 546G > T mutation at the last codon of exon2 (A upper: control, lower: patient), which creates mRNA with skipping exon 2 (B).

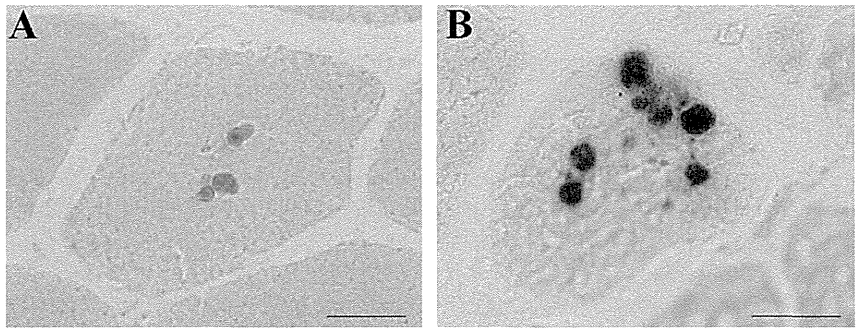

Fig. 3. Inclusions on menadione-linked α-glycerophosphate dehydrogenase (MAG) without substrate. Globular inclusions in Pompe disease (A) are only faintly stained comparing reducing bodies in reducing body myopathy with *FHL1* mutation (B). Bar = 20 μm.

rather similar [4]. However, globular inclusions showed much fainter staining on MAG without substrate than genuine reducing bodies seen in reducing body myopathy with *FHL1* mutations (Fig. 3). More importantly, ACP positivity has not been clearly described previously.

These globular inclusions are reminiscent of cytoplasmic bodies, which are nonspecific findings reflecting degeneration of the Z-disk in various neuromuscular diseases, particularly myofibrillar myopathies. However, the nature of the globular inclusions differs essentially from cytoplasmic bodies because of positive ACP staining and the lack of associated Z-disk components. Although it remains unclear how the ACP-positive globular inclusions are formed, the absence of glycogens in the globular inclusions suggest that they differ from glycogen accumulations in lysosomes. Fibers with typical vacuoles were diffusely positive for both lysosomal and autophagosomal markers as shown previously [5,6]. On the other hand, immunoreactivities of these markers accumulated more focally in fibers with inclusions. Further study should be needed to clarify what causes these pathological differences.

In conclusion, ACP-positive globular inclusions may be a hallmark of Pompe disease and a useful diagnostic marker for adult-onset Pompe disease lacking typical vacuolated fibers. Since enzyme replacement therapy is effective, albeit not fully, in adult-onset patients, early diagnosis is necessary for a better prognosis.

Ethical approval

All clinical materials used in this study were obtained for diagnostic purposes with written informed consent approved by the Ethical Committee of NCNP.

Acknowledgements

We are grateful to Satomi Mitsuhashi, Kaoru Tatezawa, Yuriko Kure, Mieko Ohnishi, and Kanako Goto (NCNP) for their technical assistance, to May Christine V. Malicdan (National Human Genome Research Institute, National Institutes of Health) for reviewing the manuscript. This study was supported by: a Grant-in-Aid for Scientific Research from Japan Society for the Promotion of Science; Research on Psychiatric and Neurological Diseases and Mental Health, Research on Measures for Intractable Diseases, Health Labor Sciences Research

Grant for Nervous and Mental Disorders (20B-12, 20B-13) from the Ministry of Health, Labor, and Welfare, and Intramural Research Grant (23-4, 23-5) for Neurological and Psychiatric Disorders from NCNP.

References

[1] Hers HG. Alpha-glucosidase deficiency in generalized glycogen storage disease (Pompe's disease). Biochem J 1963;86:11–6.
[2] Shanske S, Dimauro S. Late-onset acid maltase deficiency. Biochemical studies of leukocytes. J Neurol Sci 1981;50:57–62.
[3] Park YE, Hayashi YK, Goto K, et al. Nuclear changes in skeletal muscle extend to satellite cells in autosomal dominant Emery-Dreifuss muscular dystrophy/limb-girdle muscular dystrophy 1B. Neuromuscul Disord 2009;19:29–36.
[4] Sharma MC, Schultze C, von Moers A, et al. Delayed or late-onset type II glycogenosis with globular inclusions. Acta Neuropathol 2005;110:151–7.
[5] Raben N, Ralston E, Chien YH, et al. Differences in the predominance of lysosomal and autophagic pathologies between infants and adults with Pompe disease: implications for therapy. Mol Genet Metab 2010;101:324–31.
[6] Schoser BGH, Müller-Höcker J, Horvath R, et al. Adult-onset glycogen storage disease type 2: clinico-pathological phenotype revisited. Neuropathol Appl Neurobiol 2007;33:544–59.

ORIGINAL CONTRIBUTION

Myopathy Associated With Antibodies to Signal Recognition Particle

Disease Progression and Neurological Outcome

Shigeaki Suzuki, MD, PhD; Yukiko K. Hayashi, MD, PhD; Masataka Kuwana, MD, PhD; Rie Tsuburaya, MD, PhD; Norihiro Suzuki, MD, PhD; Ichizo Nishino, MD, PhD

Objective: To characterize the clinical course of myopathy associated with antibodies to signal recognition particle (SRP), or anti-SRP myopathy.

Design: Case series.

Setting: Keio University Hospitals and National Institute of Neuroscience, National Center of Neurology and Psychiatry, Tokyo, Japan.

Patients: We reviewed clinical features of 27 patients with anti-SRP myopathy and analyzed disease progression and neurological outcome.

Main Outcome Measures: Anti-SRP antibodies in serum were detected by RNA immunoprecipitation assay using extracts of K562 cells.

Results: Of the 27 patients, 5 (19%) showed chronic progressive muscle weakness as well as atrophy of limbs and trunk muscles from a younger age with more severe neurological outcomes compared with the other 22 patients (81%) with the subacute form.

Conclusion: A subset of patients with anti-SRP myopathy can show a chronic progressive form associated with severe clinical deficits.

Arch Neurol. 2012;69(6):728-732. Published online February 13, 2012. doi:10.1001/archneurol.2011.1728

Author Affiliations: Department of Neurology (Drs S. Suzuki and N. Suzuki) and Division of Rheumatology, Department of Internal Medicine (Dr Kuwana), Keio University School of Medicine, and Department of Neuromuscular Research, National Institute of Neuroscience, National Center of Neurology and Psychiatry (Drs Hayashi, Tsuburaya, and Nishino), Tokyo, Japan.

AUTOANTIBODIES AGAINST signal recognition particle (SRP) were first found in the serum of a patient with polymyositis and were listed as myositis-specific antibodies.[1] Myopathy associated with antibodies to SRP (anti-SRP myopathy) has recently been regarded as an immune-mediated necrotizing myopathy based on histological findings and has been clinically characterized by severe muscle weakness, marked elevation of serum creatine kinase (CK) levels, and poor response to corticosteroid therapy.[2-7] These observations were gathered mainly from patients with a clinical diagnosis of inflammatory myopathies. However, the clinical spectrum of anti-SRP myopathy may be broader.

The rapid progression of weakness is a characteristic clinical feature of anti-SRP myopathy.[2-7] The mean interval from its onset to diagnosis is 3 to 4 months, and clinical symptoms are usually progressive for 5 to 6 months.[3-5] In contrast, Dimitri et al[8] first described a 31-year-old man in whom weakness progressed for more than 3 years. Before the anti-SRP antibody was detected, he was diagnosed as having limb-girdle muscular atrophy. We also described a 32-year-old man with childhood-onset myopathy whose diagnosis alternated between inflammatory myopathy and muscular dystrophy for 21 years.[9] These results suggested that patients with anti-SRP myopathy can show chronic progression indistinguishable from muscular dystrophy. Herein, we analyzed the disease course and neurological outcomes in patients with anti-SRP myopathy.

METHODS

We chose 27 patients with myopathy with the anti-SRP antibody, including 10 previously reported cases.[9,10] The diagnosis of anti-SRP myopathy was based on clinical, electrophysiological, histopathological, and serological findings. Muscle weakness was assessed by manual muscle strength (Medical Research Council scale grade), and severe weakness was defined as grade 3 or lower. Muscle biopsy was performed in all 27 patients and showed fiber size variation as well as fiber necrosis and regeneration with or without lymphocyte infiltration. No patients had taken statins.

Anti-SRP antibodies were detected by RNA immunoprecipitation assay using extracts of K562 cells as previously described.[11] Briefly, 10 μL of serum was mixed with 2 mg of Protein A Sepharose CL-4B (Pharmacia Biotech AB) in 500 μL of immunoprecipitation buffer (10mM TRIS hydrochloride, pH 8.0, 500mM sodium chloride, 0.1% Nonidet P40) and incubated for 2 hours. After washing 3 times with immunoprecipitation buffer, antigen-bound Sepharose beads were mixed with 100 μL of K562 cell extract (6×10^6 cell equivalents per sample) for 2 hours, and 30 μL of 3M sodium acetate, 30 μL of 10% sodium dodecyl sulfate, and 300 μL of phenol:chloroform:isoamyl alcohol (50:50:1, containing 0.1% 8-hydroxyquinoline) were added to extract bound RNA. After ethanol precipitation, the RNA was resolved by using a 7M urea–8% polyacrylamide gel, and the gel was silver stained (Bio-Rad). Immunoprecipitated RNA located in the 7SL-RNA lesion was regarded as anti-SRP antibody. Other myositis-specific and myositis-associated autoantibodies were also detected by the RNA immunoprecipitation assay.

Neurological outcomes were assessed using the modified Rankin Scale (mRS).[12] This scale was principally used for evaluating function of patients with stroke; however, it was also applied to patients with myositis.[13] Neurological outcomes were divided into 3 groups: recovered, mild deficit, and severe deficit. Patients who responded optimally to the treatment and returned to their jobs (mRS score of 0-1) were defined as recovered. Patients who responded partially to treatment and resumed most activities of daily living (mRS score of 2-3) were defined as having a mild deficit. Patients who showed reworsening muscle weakness or re-elevation of serum CK levels after the treatment were also included in this group. Patients who responded minimally to the treatment and required support in daily activities (mRS score of 4) were defined as having a severe deficit.

This study was approved by the institutional review boards at Keio University and the National Center of Neurology and Psychiatry. Statistical analyses were performed using StatView version 5.0 statistical software (SAS Institute, Inc).

RESULTS

Figure 1 shows the distribution of periods between disease onset and the first examination. We divided 27 patients with anti-SRP myopathy into 2 subtypes (subacute and chronic forms) based on the clinical course. Of the 27 patients with anti-SRP myopathy in our study, 5 (19%) were considered to have the chronic form. The patients' demographic and clinical features are compared between those with the subacute and chronic forms (**Table 1**). Disease onset occurred at a younger age in those with the chronic form than in those with the subacute form (mean age, 15.4 vs 52.4 years, respectively; $P < .001$). No patients with the chronic form had a clear clinical history of antecedent infection, whereas 3 patients (14%) with the subacute form had antecedent infection. Despite a previous report,[5] seasonal occurrence was not clear in our series. Disease progression of the subacute form was usually rapid, and the mean duration between disease onset and the first examination was 3.1 months. In particular, 3 patients showed rapid disease progression in 2 to 3 weeks. In contrast, patients with the chronic form showed significantly slower progression, and the mean duration between disease onset and the first examination was 10.2 months ($P = .001$).

In our series, asymmetrical muscle involvement was seen in 2 patients, whereas the other 25 patients showed proximal-dominant symmetrical limb muscle weakness. Lower limbs were more severely affected than upper limbs. All 5 patients with the chronic form and about half of the patients with the subacute form showed severe muscle weakness and atrophy at the first examination. Several reports emphasized that dysphagia, but not dysarthria, was observed at a high frequency in 43% to 75% of patients with anti-SRP myopathy.[3,5,7] In our series, 7 patients (26%) had dysphagia and 3 (11%) reported it as the initial symptom. Previous reports also showed a high frequency of cardiac involvement,[2,5] while only 1 patient in our series had arrhythmias, which did not require treatment. Respiratory muscle involvement was detected in 3 patients. Myalgia was noted in 9 patients (36%) and tended to precede muscle weakness. Extramuscular manifestations were observed only in patients with the subacute form. Skin rash and interstitial lung disease, which were clinically suggestive of dermatomyositis, were observed in 2 and 4 patients, respectively. Serum CK levels were markedly elevated to more than 1000 IU/L (to convert to microkatals per liter, multiply by 0.0167) in all 27 patients; however, there was no difference between the subacute and chronic forms. Other autoantibodies were found in 6 patients with the subacute form, including Ro/SSA (3 patients), Th/To (1 patient), ribosome (1 patient), and U1RNP (1 patient).

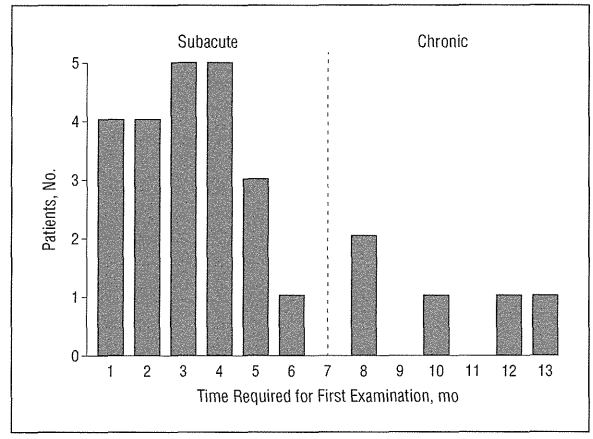

Figure 1. Period between disease onset and the first examination in 27 patients with anti–signal recognition particle myopathy. They were divided into 22 patients with the subacute form and 5 patients with the chronic form based on the clinical course.

All 27 patients were treated with oral prednisolone (1 mg/kg/d). Half of the patients were treated with additional immunosuppressive agents, including methotrexate (n = 5), azathioprine (n = 4), tacrolimus (n = 2), cyclophosphamide (n = 1), and cyclosporine (n = 1), or with intravenous immunoglobulin (n = 6). Although some patients required 2 to 3 months to respond to treatment, the patients with anti-SRP myopathy did not always respond poorly. The combination of oral prednisolone and intravenous immunoglobulin appears to be most effective for patients with the subacute form as the initial treatment. The neurological outcomes showed that 10 patients (45%) with the subacute form recovered. In contrast, all 5 patients with the chronic form had more severe neurological outcomes compared with the 22 patients with the subacute form ($P = .008$) (**Figure 2**).

Table 1. Comparison of Clinical Features Between Subacute and Chronic Forms of Anti–Signal Recognition Particle Myopathy

Clinical Feature	Patients, No. (%)		*P* Value
	Subacute (n = 22)	Chronic (n = 5)	
Age at onset, mean (range), y	52.4 (14-82)	15.4 (5-32)	<.001[a]
Female	12 (55)	3 (60)	.78[b]
Antecedent infection	3 (14)	0	.93[b]
Time required for first examination, mean (range), mo	3.1 (1-6)	10.2 (8-13)	.001[a]
Muscle weakness			
Arms < legs	16 (73)	3 (60)	.98[b]
Arms > legs	6 (27)	2 (40)	.98[b]
Severe involvement	11 (50)	5 (100)	.12[b]
Laterality	1 (5)	1 (20)	.80[b]
Facial muscle involvement	1 (5)	1 (20)	.80[b]
Bulbar sign	6 (27)	1 (20)	.81[b]
Cardiac involvement	1 (5)	0	.80[b]
Respiratory failure	3 (14)	1 (20)	.73[b]
Neck weakness	9 (41)	4 (80)	.27[b]
Muscle atrophy	10 (45)	5 (100)	.08[b]
Myalgia	8 (36)	1 (20)	.86[b]
Extramuscular involvement			
Fever	4 (18)	0	.73[b]
Skin rash	2 (9)	0	.80[b]
Arthritis	1 (5)	0	.80[b]
Raynaud phenomenon	1 (5)	0	.80[b]
Interstitial lung disease	4 (18)	0	.73[b]
Associated disorder			
Cancer	1 (9)	0	.80[b]
Rheumatic disorder	1 (9)	0	.80[b]
Serum creatine kinase, mean (range), IU/L	6101 (1149-15 585)	4190 (2465-5725)	.08[a]

SI conversion factor: To convert serum creatine kinase to microkatals per liter, multiply by 0.0167.
[a] Statistical analysis by *t* test.
[b] Statistical analysis by χ^2 test.

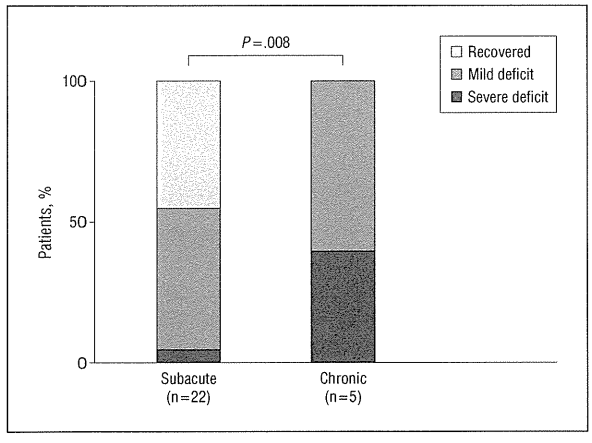

Figure 2. Neurological outcomes were assessed using the modified Rankin Scale[12] with some modifications and were compared between subacute and chronic forms of anti–signal recognition particle myopathy. The neurological outcomes were divided into recovered, mild deficit, and severe deficit. Differences between the groups were analyzed with the Mann-Whitney test. Five patients with the chronic form showed more severe outcomes than 22 patients with the subacute form (*P* = .008).

Detailed clinical features of 5 patients with the chronic form are summarized in **Table 2**. All patients had severe muscle weakness and marked atrophy in all 4 limbs and the trunk. Two patients (patients 2 and 5) noticed arm muscle weakness as the initial symptom. Importantly, scapular winging was noted in 2 patients (patients 2 and 3) at the first examination and was suspected to involve facioscapulohumeral muscular dystrophy. The serum CK level was decreased after treatment in patients with the chronic form, but muscle weakness gradually progressed and recovery of muscle strength was delayed. Three patients (patients 1, 2, and 3) became unable to walk independently, and 1 (patient 3) required mechanical ventilation. Because muscle biopsies were not suggestive of inflammatory myopathy, 1 patient (patient 3) was treated for only 3 months and 2 (patients 1 and 2) were treated after the detection of anti-SRP antibody. Of these younger patients, 2 (patients 2 and 3) became severely disabled, whereas the other 2 (patients 4 and 5) were treated soon after the muscle biopsy and responded partially to treatment.

COMMENT

There are 2 methods for detecting anti-SRP antibodies: the RNA immunoprecipitation assay we used and an immunoassay using the signal peptide–binding 54-kDa subunit of SRP (SRP54) as the antigen. Because SRP54 is regarded as the main antibody target, the immunoassay using SRP54 is easily conducted and the antibody level is also available.[1,2,14] However, epitopes of anti-SRP antibodies may also be located in other subunits of SRP proteins or 7SL-RNA.[7,15] In contrast, RNA immunoprecipitation assay, the standard method for detection of

Table 2. Clinical Features of 5 Patients With the Chronic Type of Anti–Signal Recognition Particle Myopathy

Feature	Patient No. 1[a]	2[a]	3[a]	4	5
Sex	F	F	M	F	M
Age at onset	5 y 9 mo	9 y 8 mo	10 y 2 mo	20 y 10 mo	32 y 9 mo
Initial symptoms	Frequent falls	Difficulty raising arm	Difficulty running fast	Difficulty climbing stairs	Difficulty raising his child
Weakness and atrophy	Proximal limbs (U < L); trunk	Proximal limbs (U > L); trunk; scapular winging; left dominant; myalgia	Proximal limbs (U < L); trunk; scapular winging; facial, bulbar; respiratory	Proximal limbs (U < L); trunk	Proximal limbs (U > L); trunk; strenocleidomastoideus
Serum creatine kinase, IU/L	4629	2467	4180	3951	5725
Muscle images	Atrophy in proximal limbs and trunk	Left-dominant atrophy and edematous change in proximal limbs and trunk	Atrophy and edematous change in proximal limbs and trunk	Atrophy and edematous change in proximal limbs and trunk	Atrophy and edematous change in proximal limbs and trunk
Age at muscle biopsy	6 y 5 mo	10 y 4 mo	11 y 3 mo, 16 y 6 mo	21 y 8 mo	33 y 9 mo
Muscle biopsy					
Variation in fiber size	Scattered	Scattered	Marked	Marked	Marked
Fiber necrosis and regeneration	Moderate	Marked	Marked	Scattered	Marked
Lymphocyte infiltration	None	None	None	None	Perivascular
Endomysial fibrosis	Minimal	Mild	Marked	Minimal	Mild
Age at anti-SRP antibody detection	7 y 4 mo	10 y 9 mo	32 y 6 mo	21 y 10 mo	34 y 3 mo
Age at treatment start	7 y 4 mo	10 y 9 mo	11 y 6 mo	21 y 8 mo	33 y 9 mo
Treatment	PSL, MTX, MPR	PSL, MTX, IVCY, AZA, tacrolimus	PSL (3 mo)	PSL, MPR	PSL, MTX, IVIg, tacrolimus
Age at final follow-up	9 y 3 mo	13 y 10 mo	34 y 8 mo	23 y 3 mo	35 y 6 mo
Response and neurological outcome	Partial response; progression for 2 y; relapse; MMT grade 4; Gowers sign	Minimal response; progression for 2 y; MMT grade 2-3; walking 20 m; difficulty in holding dishes	No response; progression for 3 y; recovered from mechanical ventilation; MMT grade 2-3; wheelchair use	Partial response; progression for 1 y; MMT grade 4	Partial response; progression for 1.5 y; weakness recovered; relapse

Abbreviations: AZA, azathioprine; IVCY, intravenous cyclophosphamide; IVIg, intravenous immunoglobulin; L, lower; MMT, manual muscle strength; MPR, high-dose methylprednisolone sodium succinate; MTX, methotrexate; PSL, prednisolone; SRP, signal recognition particle; U, upper.

SI conversion factor: To convert serum creatine kinase to microkatals per liter, multiply by 0.0167.

[a]These patients were previously described.[9,10]

anti-SRP antibodies, has advantages in sensitivity and specificity.[1,2,4,6,9,11] The RNA immunoprecipitation assay can recognize the conformational epitopes of SRP, although the titer of antibodies is not available. Many studies showed that anti-SRP antibodies were principally specific to myositis or necrotizing myopathy except in a few patients with systemic sclerosis or rheumatoid arthritis.[1,2,4,6,9,11] In regard to myopathies, we demonstrated that anti-SRP antibody was not detected in patients with various types of muscular dystrophy, and it was useful for the differential diagnosis of myopathies using RNA immunoprecipitation assay.[9]

Anti-SRP myopathy can show a wider variety of clinical symptoms than was previously considered. When weakness progresses rapidly, within 2 to 3 weeks, with extremely high serum CK levels (>10 000 IU/L), acute rhabdomyolysis should be differentiated.[8] When patients experience progressive weakness within 2 to 6 months[2-7] accompanied by interstitial lung disease, skin rash, or associated rheumatic disorders, polymyositis or dermatomyositis should be considered. Because skin rash is observed in approximately 10% of cases of anti-SRP myopathy in the present and previous studies,[5] anti-SRP antibodies may be also detected in patients clinically diagnosed as having dermatomyositis. In fact, Hamaguchi et al[16] reported that anti-SRP antibodies were detected in 7 of 376 patients (2%) with dermatomyositis using a similar detection method.

In our series, 5 of 27 patients with anti-SRP myopathy (19%) showed chronic progressive muscle involvement. The mean age at onset in these 5 patients was significantly younger than that of the patients with the subacute form, and patients with the chronic form showed severe weakness and atrophy in limbs and trunk muscles as well as poorer outcomes. It was speculated that the poor outcome may be partially ascribed to the delay of the first examination or anti-SRP antibodies detection. Importantly, these clinical features may indicate the possibility of muscular dystrophy rather than inflammatory myopathy,[8-10] although the disease progression was faster than occurs in muscular dystrophy. In fact, facioscapulohumeral muscular dystrophy was initially suspected in 2 patients owing to prominent shoulder-girdle weakness.[9,10]

It is well known that anti-SRP myopathy is usually resistant to treatment, resulting in severe disablement.[2-4,6,7] However, our observation suggested that patients with the subacute form had relatively good neurological outcomes. Early diagnosis by screening for anti-SRP antibodies is important for choosing intensive immunotherapy, which might contribute to better outcomes. In this regard, Hengstman et al[5] reported that the response to treatment for patients with anti-SRP myopathy did not differ significantly from that of myositis without anti-SRP antibodies. They reported that 75% of patients with anti-SRP myopathy could walk without any assistance after treatment. The severe outcomes of anti-SRP myopathy described in the previous studies may be attributable partly to results for patients with the chronic form. Rituximab therapy is potentially effective for patients with the chronic form.[7] Based on these findings, it may be useful to divide patients by disease progression to predict the neurological outcome.

An apparent question about the relationship between anti-SRP antibodies and muscle involvement is whether the anti-SRP antibodies themselves have any pathogenic effect against muscle. This hypothesis may be supported by several lines of data: (1) anti-SRP antibodies purified from patients' serum samples can inhibit the in vitro translocation of secretory proteins into endoplasmic reticulum[17]; (2) the levels of anti-SRP54 autoantibodies are closely associated with the levels of myolysis[14]; and (3) the removal of anti-SRP antibodies by plasma exchange improves muscle strength.[14,18] Nevertheless, the causal relationship between anti-SRP antibodies and muscle involvement is still not established, and further experiments such as passive transfer to animals are necessary to elucidate the pathogenesis of anti-SRP antibodies.

In conclusion, anti-SRP myopathy can show quite variable disease progression and neurological outcomes.

Accepted for Publication: August 23, 2011.
Published Online: February 13, 2012. doi:10.1001/archneurol.2011.1728
Correspondence: Shigeaki Suzuki, MD, PhD, Department of Neurology, Keio University School of Medicine, 35 Shinanomachi, Shinjuku-ku, Tokyo 160-8582, Japan (sgsuzuki@z3.keio.jp).
Author Contributions: Dr S. Suzuki had full access to all of the data in the study and takes responsibility for the integrity of the data and the accuracy of the data analysis. *Study concept and design:* S. Suzuki, Hayashi, and Nishino. *Acquisition of data:* S. Suzuki and Tsuburaya. *Analysis and interpretation of data:* S. Suzuki, Hayashi, Kuwana, and N. Suzuki. *Drafting of the manuscript:* S. Suzuki and Hayashi. *Critical revision of the manuscript for important intellectual content:* Kuwana, Tsuburaya, N. Suzuki, and Nishino. *Statistical analysis:* S. Suzuki. *Obtained funding:* S. Suzuki, Hayashi, and Nishino. *Administrative, technical, and material support:* Hayashi, Kuwana, Tsuburaya, and N. Suzuki. *Study supervision:* Nishino.
Financial Disclosure: None reported.

Funding/Support: This work was supported by grant 18790601 from the Japanese Ministry of Education, Science, Sports, and Culture, by a Neuroimmunological Disease Research Committee grant from the Japanese Ministry of Health, Labour, and Welfare, by a Grant-in-Aid for Scientific Research from the Japan Society for the Promotion of Science, by Health Labour Sciences Research Grant 20B-12, 20B-13 for Research on Psychiatric and Neurological Diseases and Mental Health, Research on Measures for Intractable Diseases, and Research on Nervous and Mental Disorders from the Ministry of Health, Labor, and Welfare, and by Intramural Research Grant 23-4, 23-5, 23-6 for Neurological and Psychiatric Disorders at the National Center of Neurology and Psychiatry.

REFERENCES

1. Reeves WH, Nigam SK, Blobel G. Human autoantibodies reactive with the signal-recognition particle. *Proc Natl Acad Sci U S A.* 1986;83(24):9507-9511.
2. Targoff IN, Johnson AE, Miller FW. Antibody to signal recognition particle in polymyositis. *Arthritis Rheum.* 1990;33(9):1361-1370.
3. Miller T, Al-Lozi MT, Lopate G, Pestronk A. Myopathy with antibodies to the signal recognition particle: clinical and pathological features. *J Neurol Neurosurg Psychiatry.* 2002;73(4):420-428.
4. Kao AH, Lacomis D, Lucas M, Fertig N, Oddis CV. Anti-signal recognition particle autoantibody in patients with and patients without idiopathic inflammatory myopathy. *Arthritis Rheum.* 2004;50(1):209-215.
5. Hengstman GJ, ter Laak HJ, Vree Egberts WT, et al. Anti-signal recognition particle autoantibodies: marker of a necrotising myopathy. *Ann Rheum Dis.* 2006;65(12):1635-1638.
6. Takada T, Hirakata M, Suwa A, et al. Clinical and histopathological features of myopathies in Japanese patients with anti-SRP autoantibodies. *Mod Rheumatol.* 2009;19(2):156-164.
7. Valiyil R, Casciola-Rosen L, Hong G, Mammen A, Christopher-Stine L. Rituximab therapy for myopathy associated with anti-signal recognition particle antibodies: a case series. *Arthritis Care Res (Hoboken).* 2010;62(9):1328-1334.
8. Dimitri D, Andre C, Roucoules J, Hosseini H, Humbel RL, Authier FJ. Myopathy associated with anti-signal recognition peptide antibodies: clinical heterogeneity contrasts with stereotyped histopathology. *Muscle Nerve.* 2007;35(3):389-395.
9. Suzuki S, Satoh T, Sato S, et al. Clinical utility of anti-signal recognition particle antibody in the differential diagnosis of myopathies. *Rheumatology (Oxford).* 2008;47(10):1539-1542.
10. Suzuki S, Ohta M, Shimizu Y, Hayashi YK, Nishino I. Anti-signal recognition particle myopathy in the first decade of life. *Pediatr Neurol.* 2011;45(2):114-116.
11. Okada N, Mimori T, Mukai R, Kashiwagi H, Hardin JA. Characterization of human autoantibodies that selectively precipitate the 7SL RNA component of the signal recognition particle. *J Immunol.* 1987;138(10):3219-3223.
12. van Swieten JC, Koudstaal PJ, Visser MC, Schouten HJ, van Gijn J. Interobserver agreement for the assessment of handicap in stroke patients. *Stroke.* 1988;19(5):604-607.
13. Danieli MG, Calcabrini L, Calabrese V, Marchetti A, Logullo F, Gabrielli A. Intravenous immunoglobulin as add on treatment with mycophenolate mofetil in severe myositis. *Autoimmun Rev.* 2009;9(2):124-127.
14. Benveniste O, Drouot L, Jouen F, et al. Correlation of anti-signal recognition particle autoantibody levels with creatine kinase activity in patients with necrotizing myopathy. *Arthritis Rheum.* 2011;63(7):1961-1971.
15. Satoh T, Okano T, Matsui T, et al. Novel autoantibodies against 7SL RNA in patients with polymyositis/dermatomyositis. *J Rheumatol.* 2005;32(9):1727-1733.
16. Hamaguchi Y, Kuwana M, Hoshino K, et al. Clinical correlations with dermatomyositis-specific autoantibodies in adult Japanese patients with dermatomyositis: a multicenter cross-sectional study. *Arch Dermatol.* 2011;147(4):391-398.
17. Römisch K, Miller FW, Dobberstein B, High S. Human autoantibodies against the 54 kDa protein of the signal recognition particle block function at multiple stages. *Arthritis Res Ther.* 2006;8(2):R39.
18. Arlet JB, Dimitri D, Pagnoux C, et al. Marked efficacy of a therapeutic strategy associating prednisone and plasma exchange followed by rituximab in two patients with refractory myopathy associated with antibodies to the signal recognition particle (SRP). *Neuromuscul Disord.* 2006;16(5):334-336.

Journal of the Neurological Sciences xxx (2012) xxx–xxx

Contents lists available at SciVerse ScienceDirect

Journal of the Neurological Sciences

journal homepage: www.elsevier.com/locate/jns

A novel mutation in SCN4A causes severe myotonia and school-age-onset paralytic episodes

Harumi Yoshinaga [a,*], Shunichi Sakoda [b], Jean-Marc Good [c], Masanori P. Takahashi [c], Tomoya Kubota [c], Eri Arikawa-Hirasawa [d], Tomohiko Nakata [e], Kinji Ohno [e], Tetsuro Kitamura [f], Katsuhiro Kobayashi [a], Yoko Ohtsuka [a]

[a] Department of Child Neurology, Okayama University Graduate School of Medicine, Dentistry, and Pharmaceutical Sciences, Okayama, Japan
[b] Department of Neurology, Kagoshima University Graduate School of Medical and Dental Sciences, Medical School, Kagoshima, Japan
[c] Department of Neurology, Osaka University Graduate School of Medicine, Osaka, Japan
[d] Department of Neurology, Juntendo University School of Medicine, Tokyo, Japan
[e] Division of Neurogenetics, Center for Neurological Diseases and Cancer, Nagoya University Graduate School of Medicine, Aichi, Japan
[f] Department of Pediatrics, Nipponkokan Fukuyama Hospital, Hiroshima, Japan

ARTICLE INFO

Article history:
Received 27 June 2011
Received in revised form 30 November 2011
Accepted 22 December 2011
Available online xxxx

Keywords:
Channelopathy
Na channel
Skeletal muscle
Activation
Slow inactivation
Schwarz–Jampel syndrome
SCN4A

ABSTRACT

Mutations in the pore-forming subunit of the skeletal muscle sodium channel (*SCN4A*) are responsible for hyperkalemic periodic paralysis, paramyotonia congenita and sodium channel myotonia. These disorders are classified based on their cardinal symptoms, myotonia and/or paralysis. We report the case of a Japanese boy with a novel mutation of *SCN4A*, p.I693L, who exhibited severe episodic myotonia from infancy and later onset mild paralytic attack. He started to have apneic episodes with generalized hypertonia at age of 11 months, then developed severe episodic myotonia since 2 years of age. He presented characteristic generalized features which resembled Schwarz–Jampel syndrome. After 7 years old, paralytic episodes occurred several times a year. The compound muscle action potential did not change during short and long exercise tests. Functional analysis of the mutant channel expressed in cultured cell revealed enhancement of the activation and disruption of the slow inactivation, which were consistent with myotonia and paralytic attack. The severe clinical features in his infancy may correspond to myotonia permanence, however, he subsequently experienced paralytic attacks. This case provides an example of the complexity and overlap of the clinical features of sodium channel myotonic disorders.

1. Introduction

To date, over 40 different mutations causing Na channelopathies of the skeletal muscle have been reported in *SCN4A* gene, which encodes for the pore-forming alpha-subunit of skeletal muscle sodium channel [1,2]. The Na channelopathies of the skeletal muscle are clinically classified into hyperkalemic periodic paralysis, paramyotonia congenita, or sodium channel myotonia on the basis of their clinical phenotype. However, phenotypic variability and marked overlap in symptoms have been reported [3–6]. The cases with severe phenotype in the neonatal period highlight the high clinical variability of sodium channelopathies [7,8]. The electrophysiological studies using heterologously expressed channels have shown that the missense mutations produces a gain-of-function defect of the fast gating such as disrupted fast inactivation and enhanced activation, which should result in increased excitability of the muscle membrane. It has been revealed that not only the defect of fast gating but also that of slow inactivation predisposes to paralytic attack, one of the clinical features of Na channelopathies [9,10].

In this report, we present a Japanese boy with skeletal dysplasia who exhibited very severe myotonia in infancy and mild paralytic attack after seven years of age. We identified a novel mutation in the intracellular loop linking segments 4–5 of domain II in *SCN4* and found that the heterologously expressed mutant channel showed enhancement of the activation and disruption of the slow inactivation.

2. Case report

2.1. Clinical features

The patient was delivered naturally and without complications. There is no family history of neuromuscular disease. Seven days after birth, he experienced transient breath-holding episodes with generalized muscle stiffness and facial pallor while crying. At 11 months of age, 30-second-long episodes of apnea arose with

* Corresponding author at: Shikatacho 2-5-1 Department of Child Neurology, Okayama University Graduate School of Medicine, Dentistry, and Pharmaceutical Sciences, Okayama 700-8558 Japan. Tel.: +81 86 235 7372; fax: +81 86 235 7377.
E-mail address: magenta@md.okayama-u.ac.jp (H. Yoshinaga).

0022-510X/$ – see front matter © 2012 Elsevier B.V. All rights reserved.
doi:10.1016/j.jns.2011.12.015

Please cite this article as: Yoshinaga H, et al, A novel mutation in SCN4A causes severe myotonia and school-age-onset paralytic episodes, J Neurol Sci (2012), doi:10.1016/j.jns.2011.12.015

generalized hypertonia; these episodes were so severe that epileptic seizures were once suspected, but ictal EEG recordings did not indicate that this was the case. These episodes spontaneously disappeared, but at the age of two, the patient started to present daily fluctuating myotonia. The patient presented with a mask-like face with blepharospasm, grip myotonia, and dysarthria. These episodic myotonic attacks persisted for several minutes, hours, or even days, with fluctuation and created difficulties in standing, walking and upper-limb mobility. The symptoms seemed to be aggravated by cold (and were relieved during febrile illness) and fatigue, but not by potassium intake or exercise. The CK value fluctuated between 200 and 1000+ and tended to be high during myotonic attacks.

Fig. 1 depicts a generalized inter-episode feature when he was 5 years and 8 months old. Parental consent to present the photograph in Fig. 1 was obtained. He was of Herculean stature and exhibited several characteristic features, such as low-set ears, epicanthic folds, upturned nose, a long philtrum, puckered lips, short neck, hypertropic thighs, atrophic shoulder girdle muscles, pigeon breast, and joint contracture of the elbow. Accordingly, he was initially suspected as having a myogenic type of Schwarz–Jampel syndrome [4,11]. However, immunofluorescence stain for perlecan was normal in biopsied muscle and the histology revealed a nonspecific myopathic change with increased fiber variability. Acetazolamide, mexiletine, and phenytoin had some effect on his myotonic attacks. When these medications were discontinued on the day he underwent generalized anesthesia for the muscle biopsy, he experienced a very severe myotonic attack that involved the respiratory muscle.

Fig. 1. The patient at 5 years and 8 months of age. Note his Herculean stature and hypertrophic thighs.

After 7 years and 8 months of age, paralytic episodes appeared that occurred several times a year thereafter, even in hot summertime temperatures. He complained of muscle weakness lasting from hours to several days at a time. His mother observed that his thighs become unusually soft during episodes. Neither exercise nor cooling brought about his episodic weakness.

2.2. Clinical electrophysiological analysis

Needle electromyography revealed diffuse continuous myotonic discharges accentuated by needle displacement with dive bomber sounds. Analysis of the compound muscle action potential (CMAP) amplitude before and after short or long exercise revealed no significant change [12]. Muscle cooling did not affect the CMAP either [13].

2.3. DNA analysis

Since there was no expansion of the repeat length at the DM1 locus with Southern blot, we analyzed the nucleotide sequence of *SCN4A* and *CLCN1* genes. Written informed consent was obtained from the parents for the mutation screening. This study was approved by the ethics committee of Kagoshima University Graduate School of Medical and Dental Sciences. Nucleotide sequence analysis of the patient's DNA showed a transition of A to C at the nucleotide in position 2077 (c.2077A>C) in *SCN4A* resulting in the substitution of isoleucine to leucine at amino acid in position 693 (p.I693L) (Fig. 2A). This mutation was not found in the DNA of the parents, both of whom were clinically non-affected. No mutations of *CLCN1* genes were identified by sequencing analysis.

Furthermore, the possibility of Schwarz–Jampel syndrome was excluded by re-sequencing all the exons and the flanking intronic regions of *HSPG2*. We enriched exonic fragments using the SureSelect Human All Exon v2 kit (Agilent, CA, USA), and read 50-bp fragments with the ABI SOLiD 4 sequencer (Applied Biosystems, CA, USA). We mapped 56,007,335 tags (89% of total tags) to human genome GRCh37.3/hg19 with BioScope 1.3.1 (Applied Biosystems), and read 2338 Mbp. Detection of SNVs with Avadis NGS (Strand Life Sciences, Bangalore, India) using default parameters revealed three homozygous missense SNPs that were all registered in dbSNP134 without any reference to clinical relevance (W71S, rs2254357, global minor allelic frequency (GMAF) = 0.475; G242V, rs2254358, GMAF = 0.476; and N765S, rs989994, GMAF = 0.068).

2.4. Sodium channel functional study

We cultured human embryonic kidney (HEK) cells and transfected them with wild-type or mutant human sodium channel constructs as previously described [14]. Na + currents were recorded by the conventional whole-cell patch clamp technique. As shown in Fig. 3A, the mutant channels were consistently activated at more hyperpolarized voltages than the wild-type channels. To further investigate this phenomenon, the normalized sodium conductance at each measured peak current was calculated and plotted against the corresponding voltage. There was a marked shift towards hyperpolarized voltages in the activation curve of p.I693L mutant channels indicating an enhancement of the activation (Fig. 3B. Table 1).

Please cite this article as: Yoshinaga H, et al, A novel mutation in SCN4A causes severe myotonia and school-age-onset paralytic episodes, J Neurol Sci (2012), doi:10.1016/j.jns.2011.12.015